TALLINNA TEHNIKAÜLIKOOL
MEHAANIKATEADUSKOND

Materjalitehnika instituut
Metallide tehnoloogia õppetool

MTT70LT

Pavel Lahno

VALAMISTEHNOLOOGIA ABIL SAADUD KERAAMILISTE MATERJALIDE EROSIOONIKINDLUS

Autor taotleb
tehnikateaduse magistri
akadeemilist kraadi

Tallinn
2015

AUTORIDEKLARATSIOON

Deklareerin, et käesolev lõputöö on minu iseseisva töö tulemus.

Esitatud materjalide põhjal ei ole varem akadeemilist kraadi taotletud.

Töös kasutatud kõik teiste autorite materjalid on varustatud vastavate viidetega.

Töö valmis.. juhendamisel

"......."....................201….a.

Töö autor

.... allkiri

Töö vastab magistritööle esitatavatele nõuetele.

"......."....................201….a.

Juhendaja

.... allkiri

Lubatud kaitsmisele.

.... eriala/õppekava kaitsmiskomisjoni esimees

"......."....................201… a.

.... allkiri

TALLINNA TEHNIKAÜLIKOOL
MEHAANIKATEADUSKOND

Department of Materials Engineering
Chair of Metals Technology

MTT70LT

Pavel Lahno

EROSION RESISTANCE
OF CAST CERAMIC MATERIALS

Author applies for degree of Master of Technical Sciences (M.Sc.)

Tallinn
2015

TTÜ materjalitehnika instituut

Metallide tehnoloogia õppetool

MAGISTRITÖÖ ÜLESANNE

2015 aasta, kevade semester

Üliõpilane: Pavel Lahno, 122094
Õppekava: MATM02/11
Eriala: Tootmistehnika
Juhendaja: Maksim Antonov, Vanemteadur, MTI, TTÜ
Konsultandid: Janis Baroninš, Doktorant, MTI, TTÜ

MAGISTRITÖÖ TEEMA:
(eesti keeles) Valamistehnoloogia abil saadud keraamiliste materjalide erosioonikindlus
(inglise keeles) Erosion resistance of cast ceramic materials

Lõputöös lahendatavad ülesanded ja nende täitmise ajakava:

Nr	Ülesande kirjeldus	Täitmise tähtaeg
1.	Kirjanduse lugemine (kulumine, keraamilised materjalid)	01.04.2015
2.	Katsekehade ettevalmistamine	01.01.2015
3.	Katsetamine	01.05.2015
4.	Lõputöö kirjutamine	01.06.2015

Lahendatavad insenertehnilised ja majanduslikud probleemid: Valitakse materjal uue erosioonkatsemasina küttespiraalide kinnitamiseks

Täiendavad märkused ja nõuded: puuduvad
Töö keel: inglise keel
Kaitsmistaotlus esitada hiljemalt: 12/05/2015   **Töö esitamise tähtaeg:** 01/06/2015

Üliõpilane: P. Lahno   /allkiri/ ………..   kuupäev………

Juhendaja: M. Antonov   /allkiri/ ……….   kuupäev………

CONTENT

APPENDICES

Appendix 1. Drawings of holder construction for specimens

EESSÕNA

Tavaliselt teaduslikus töös on näha mitme isiku panust ning teatud töö ei ole erand. Esiteks ma tahaks tänada Maksim Antonovi (Triboloogia ja materjali katsetuste teaduslaboratooriumi juhataja) tema isikliku panuse, entusiasmi ja juhendamise eest testi ettevalmistamisel ja läbiviimisel. Tahaks hinnata Mr. Janis Baroninš panust testi tulemuste detailsel uuringul ja analüüsimisel, esitatud uue erosiooni testeri 3D joonist. Roman Ivanovi tema poolt abi osutamise eest proovikehade loomisel. Lisaks tahaks tänada Tallinna Tehnikaülikooli Materjalitehnika instituut, et oli antud võimalus kasutada vajaliku tehnikat proovikehade loomise ja nende testimise jaoks.

ACKNOWLEDGEMENTS

1. INTRODUCTION

Erosion is one of wear processes that occurs in gas, liquid or atmosphere, by the repeated impact of solid particles against the surface of material at any significant velocity. Repeated erodent impacts during a long period of time lead to erosion damage. The results of this repeated action is the loss of material. Due to variation of conditions there are many types of erosive wear. Such type as solid particle erosion will be described in theory in the first part of this work. Like other wear processes, erosion includes a lot of influence factors. Also materials have different behaviour during erosion. In common with other forms of wear, mechanical strength or hardness does not guarantee wear resistance and a detailed study of material characteristics is required for wear minimization. It can bring serious damage to engineering systems, including steam and jet turbines, pipelines and valves carrying particulate matter, and fluidized bed combustion systems. Even in space particle erosion can be found. A low earth orbit satellite provides an example of erosive wear by minute particles. The satellite is a subject to erosion by impacting oxygen and nitrogen atoms from the outer atmosphere and this eventually causes degradation of the satellite casing [1, 2, 3, 4].

This work is to be unique in a way of new combinations of materials that were presented for producing ceramic and other composite materials, that nobody had investigated before. Main materials used were: castable ceramics, basalt, liquid glass. These materials have many advantages, because of their cost and prevalence. Results obtained in this work give knowledge of using basalt and liquid glass, and will be useful in fabricating of new ceramic materials. Moreover tested ceramic materials based on Cotronics base can be used as electric insulator for high temperature applications.

Ceramics are regarded as interesting materials for applications in a wide range of temperatures due to their good thermal and mechanical properties. Ceramics have a high price, that is caused by difficulties of their manufacture and fabricating parts from them. Quite often it is necessary to obtain complex shaped ceramic products such as restorative materials, irregular shape protective or bearing materials for ovens, thermo barriers, electro isolators, artificial bones etc. Usually it is technologically difficult to apply high temperature and high pressure for productions of these materials. Quality control is difficult and very important in the consistency of results in application. Ceramic parts have to be machined from their moulded or sintered shape to the final shape by time consuming and expensive grinding operations. Special techniques are required to eliminate imbedded debris from

grinding which can have disastrous results when it becomes loose in the operating system. As a result of the above problems associated with fabrication of ceramic parts, ceramic coatings are finding greater usage as they are developed. In this way, the bulk of a part can be made of a relatively inexpensive metal alloy and the wear surface then coated with the appropriate ceramic material [5].

The aims of this work are:

1. To test a new method of specimens fastening for elevated temperature erosion testing.
2. To fabricate castable ceramics.
3. To test fabricated specimens in conditions of solid particle erosion.
4. To compare new materials with commercial analogues.
5. To define material that can be used in new model of erosion tester as support of heating elements.

For comparing specimens that will be produced during this work with commercial analogues and identifying erosion rate, calculations based on changing in mass of samples will be taken. Work is divided into two parts: theory and practice. Second part is the main part that consists of 3 subparts. It is expected that results of this work will be also published as an article.

2. LITERATURE REVIEW

2.1. Wear mechanism of ductile materials

The cutting process attributes to particles striking the solid surface at a low angle and scratching out some material from the surface. This mechanism leads to the formation of "lips" at the edges of impact craters, and their removal by other particles impacting nearby. This affect on the surface with heating effect, that leads to plastic flow of the material and consequently influences the microstructure of the stressed material. Adhesive forces are also involved in this mechanism. Their evidence proves forming of overhanging "lips" at the edges of the crater. The removal can easily occur in multiple impact situations by subsequent impinging particles. Mechanism of mictrocutting or microploughing only takes place at small angles, less than 40° particularly. Further takes place formation of thin platelets, that is typical feature of erosion under high angles with round particles. Erosive wear is associated with the detachment by plastic rupture of material displaced from the impact site into raised crater rims and "lips" although each impact displaces material from the indentation formed, it will often not become detached as wear debris until it has experienced several cycles of plastic deformation and become severely work-hardened. Mechanism of erosion of ductile materials with low angle of impingement is shown in Figure 1. Mechanism of erosion of ductile materials with high angle of impingement is shown in Figure 2 [6, 7].
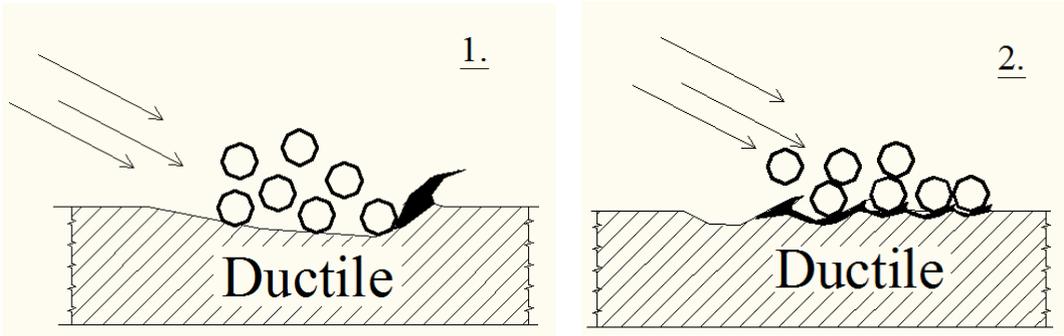
Figure 1. Mechanism of erosion of ductile materials at low angles[8]:

1) microcutting or microploughing, extrusion of material to the side in front of the particles, formation of a "lips" at the end of the impact crater

2) removal of "lips" from the end of the impact crater
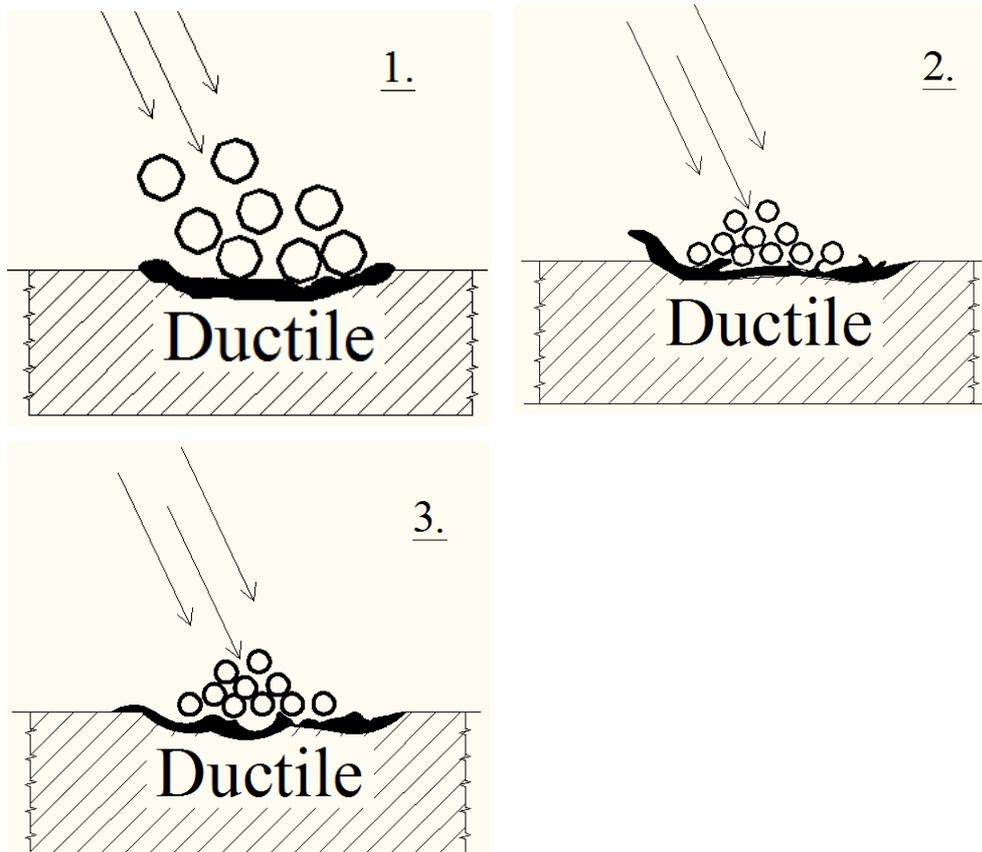
Figure 2. Mechanism of erosion of ductile materials at high angles [8]:

1) plastic deformation of the metal surface

2) formation of craters with "lips" at the edges

3) removal from the the edge of craters due to repeated impact

2.2. Wear mechanism of brittle materials

Brittle fracture or cracking of surface becomes important with increasing impingement angle, particle size, particle velocity and increasing brittleness of material. Repeated loading cycles by multiple impact of particles promotes the formation of cracks on surface or subsurface. Repeated cracking leads to flaking of material. Mechanism of erosion of brittle materials is shown at Figure 3 [9].
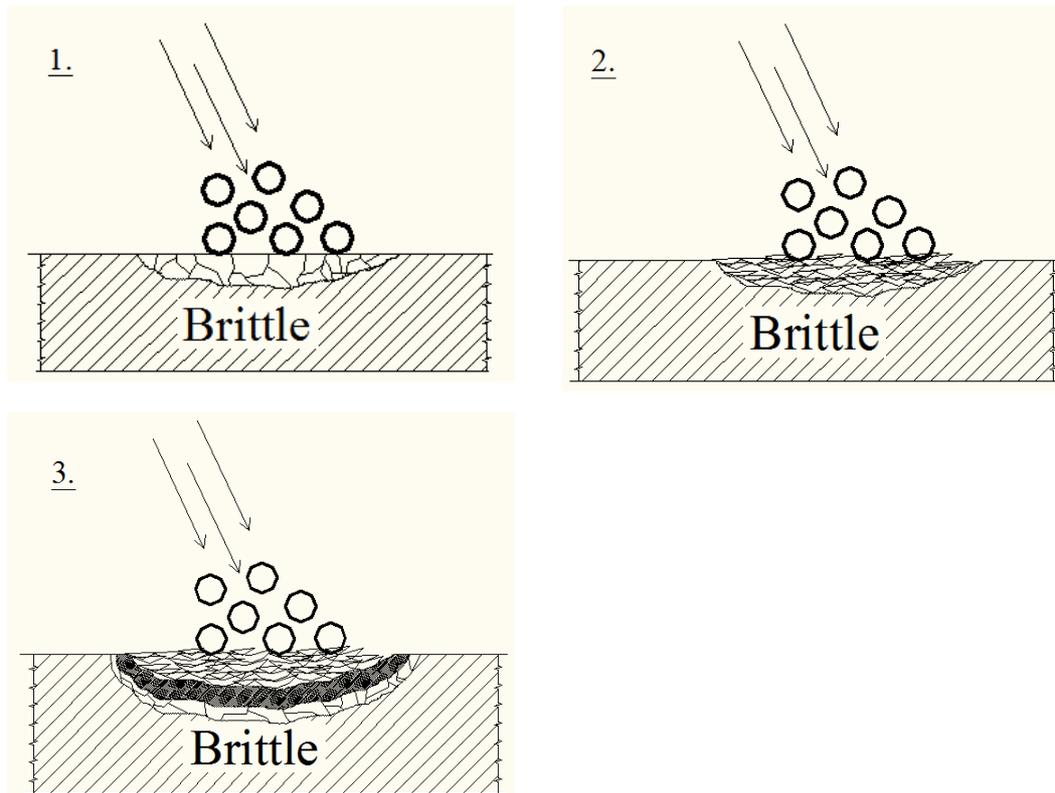
Figure 3. Mechanism of erosion of brittle materials [8]:

1) surface cracking

2) surface and subsurface fatigue cracks due to repeated impact

3) formation of thin platelets due to extrusion and forging by repeated impact, formation of new cracks on underlying material

2.2.1 Formation of cracks

Brittle materials like ceramics have a different behaviour in a way of cracking formation depending on particle shape and hardness. Rounded and soft particles cause conical Hertzian fractures. Hertzian cone cracks arise rapidly outside the contact circle, when the normal load W reaches a critical value. Scheme of Hertzian cracks formation is shown in Figure 4 [10].
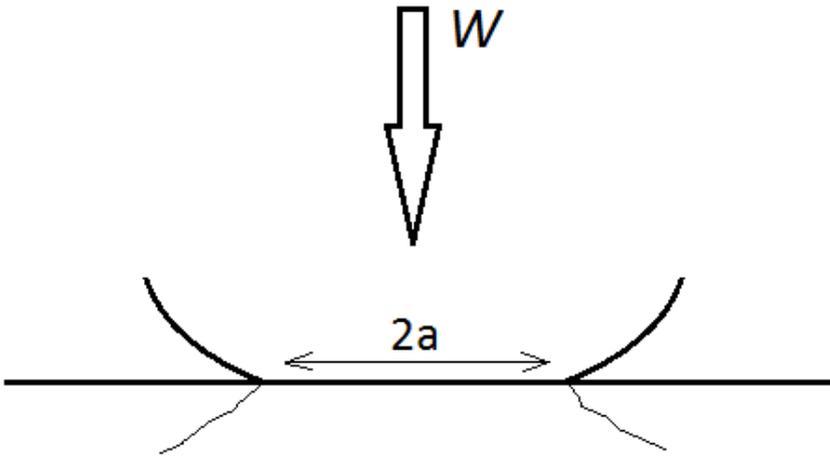
Figure 4. The geometry of Hertzian crack formed by particle loaded normally on the plane surface of a brittle material. *a*-the radius of contact circle; *W*-normal load [10]

Hard and angular particles provide cracks which are totally different from Hertzian cracks. At the point of contact can occur plastic deformation and cracks of a different geometry, which can lead to wear. Possible steps of crack evolution are shown on Figure 5 [11].
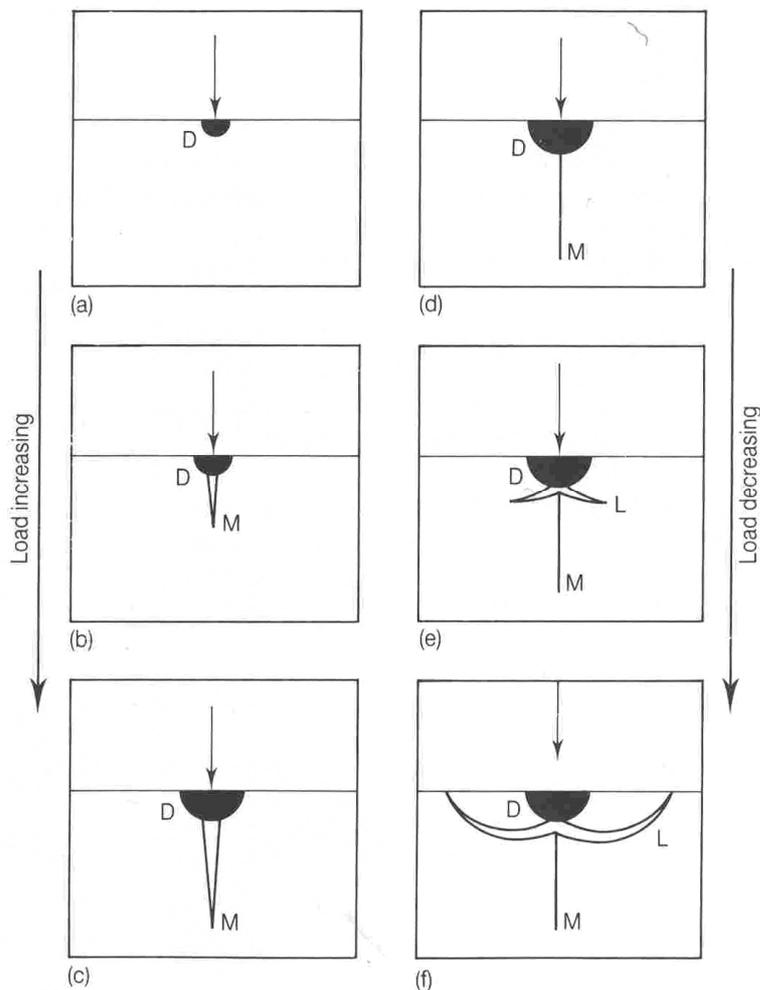
Figure 5. Scheme showing crack formation by hard and/or angular particles erosion in a brittle material. The zone of deformed material is filled by black color. When the load increases to a critical value from (a) to (c), stresses across the vertical mid-plane initiate a median crack *M*. Medial crack are closed if the load begins to reduce from (d) to (f), with simultaneous formation and growth of lateral cracks *L*. Residual elastic stresses, caused by the relaxation of the deformed material around the region of contact, provide for lateral cracks [12]

2.3. Effect of erosion on surface

Each particle causes partial abrasive wear on the impacted surface during the short time of contact. When the particle bounces, the top surface of the material adheres to the particle surface and is carried away by the mechanism of adhesive wear. Depending on the speed of impact, partial melting of the surface can be generated. The series of the fine impacts by the continuous flow of particles generate fatigue wear by introducing cracks in the surface and the subsurface. Formation of the oxide film begins if the temperature of the surroundings is high enough to cause extensive oxidation on the impacted surface. Rise of temperature occurs due to high impact energies and friction forces induced by adhesion between the particles and the surface. Effect of erosion on surface is schematically presented in Figure 6 [8, 13].
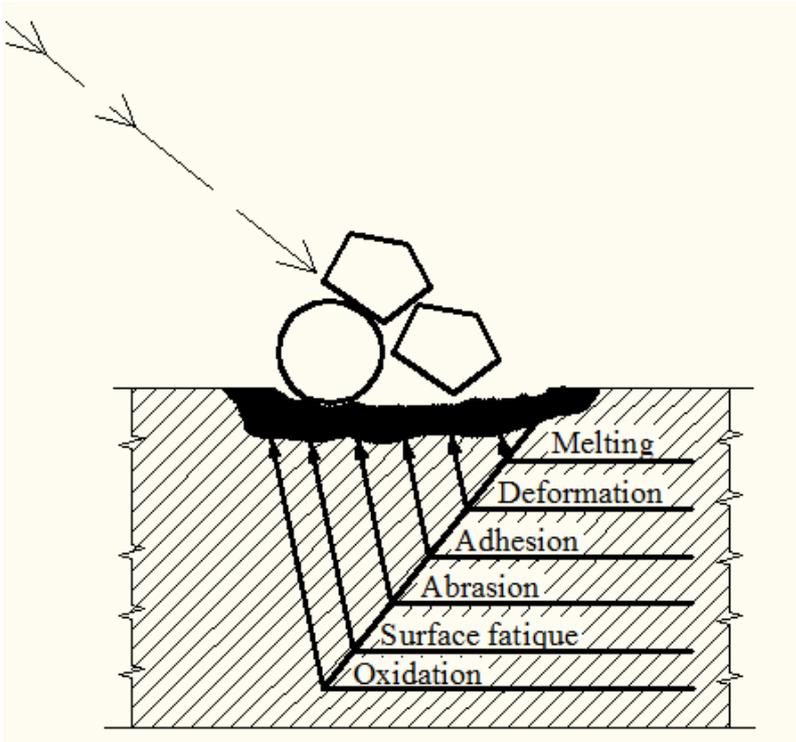
Figure 6. Complex of reactions in case of erosion

2.4. Solid particle erosion factors

Solid particle erosion has to be considered as a complex phenomena that involves many influence factors. In erosion several forces of different origins may act on a particle in contact with a solid surface. Presence of a flowing fluid will cause drag. Under some conditions, gravity may be important. The dominant force on an erosive particle, which is mainly responsible for decelerating it from its initial impact velocity, is usually the contact force exerted by the surface. All forces and factors influence on erosion are illustrated in Figure 7 [13].
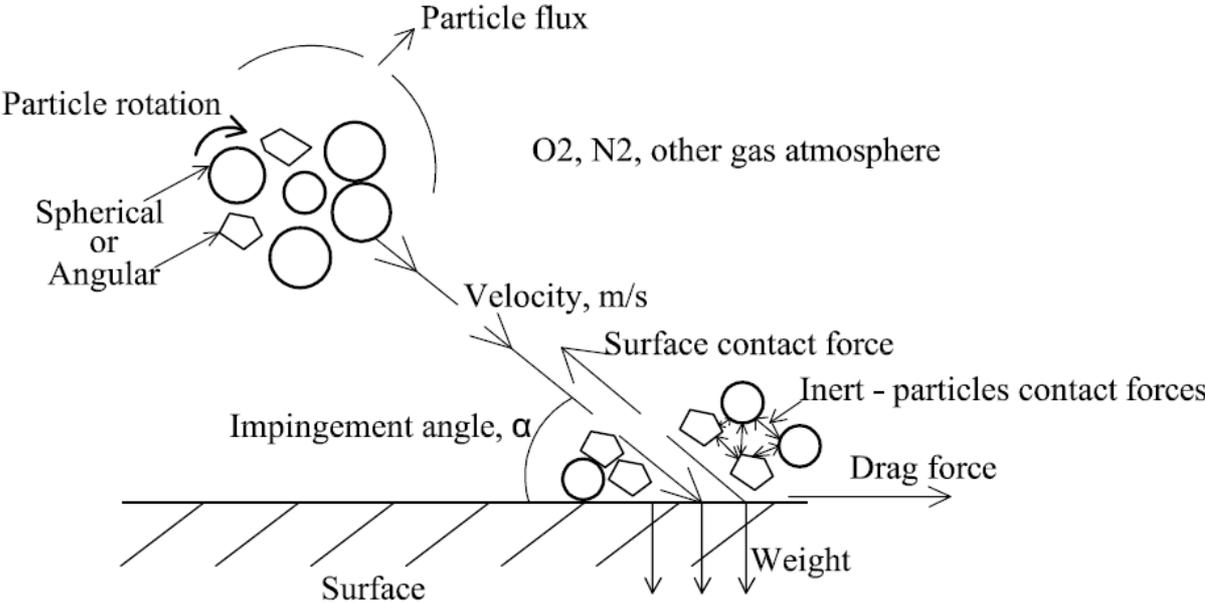
Figure 7. Scheme showing forces which can act on a particle in contact with a solid surface [14]

2.4.1. Particle speed

The speed of the erosive particles has a strong effect on the wear process. If the speed is very low then stresses at impact are insufficient for plastic deformation of the material. When the speed is increased it is possible for the eroded material to deform plastically on a particle impact. In this regime, which is quite common for many engineering components, wear may occur by repetitive plastic deformation. Impingement velocities usually range from 15 to 170 metres per second. The relationship between the wear rate and impact velocity for ductile and brittle materials is shown in Figure 8 [13, 15].
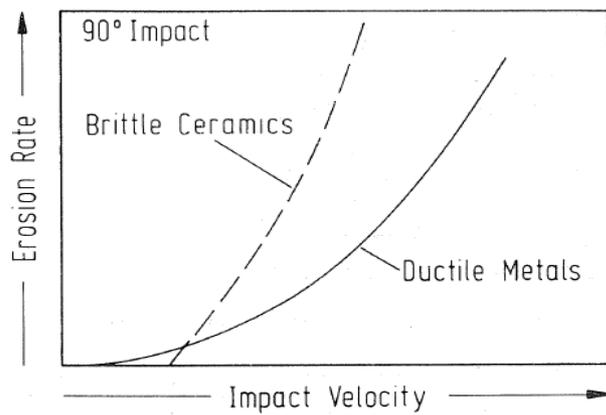
Figure 8. Effect of impact velocity on erosion rate of various materials [13]

2.4.2. Particle shape

According to visual appearance of particles these can be classified as 'spherical', 'semi-rounded', 'semi-angular' or 'angular' (see Figure 9). Such a description is subjective, especially when the gradation of the degree of angularity is sought. If the eroding particles are blunt or spherical then thin plates of worn material form on the worn surface as a result of extreme plastic deformation. Sharp particles can cause cutting or brittle fragmentation. Sharp or angular particles generally produce radial cracks, which lie perpendicular to the surface and are semicircular in shape, and which form during loading. Upon unloading, the stresses generated by the plastically compressed zone cause the formation of lateral vent cracks approximately parallel to the surface. Even if the particle is hard but relatively blunt then it is unlikely to cause severe erosive wear. A blunt particle has a mostly curved surface approximating to a spherical shape while a sharp particle consists of flat areas joined by corners with small radii which are critical to the process of wear [16, 17].
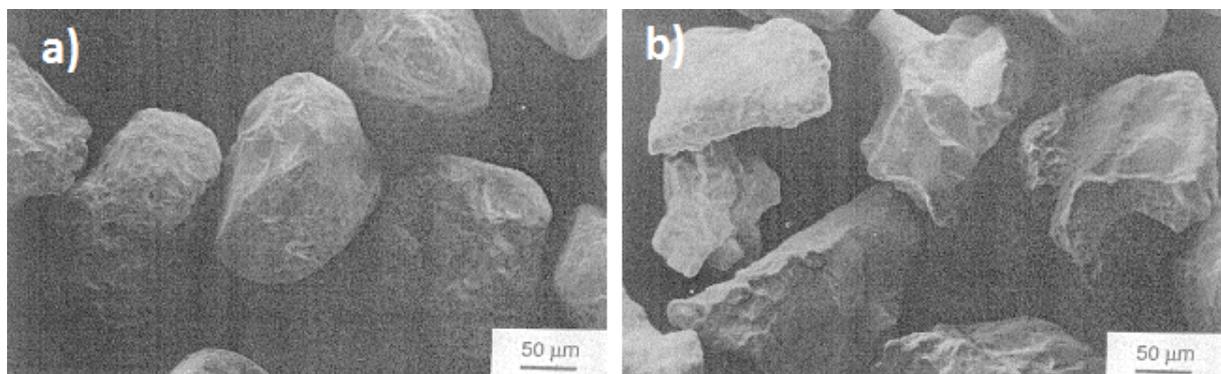
Figure 9. SEM micrographs of silica particles: a) rounded and b) angular [14]

17

In case of ductile materials spherical particles cause such type of cutting like ploughing, kind of abrasion. Ploughing is related to displacing material to the side and in front of the particle (see Figure 10). Further impacts on the neighbouring areas lead to the detachment of material from the side of the crater or from the terminal "lip". Angular particles moving forwards during impact make a crater of impact more deep and "lips" bigger. However, angular particles moving backwards during impact make a smaller crater of impact and no "lips". Scheme of such types is presented in Figure 11 and in Figure 12 [10].
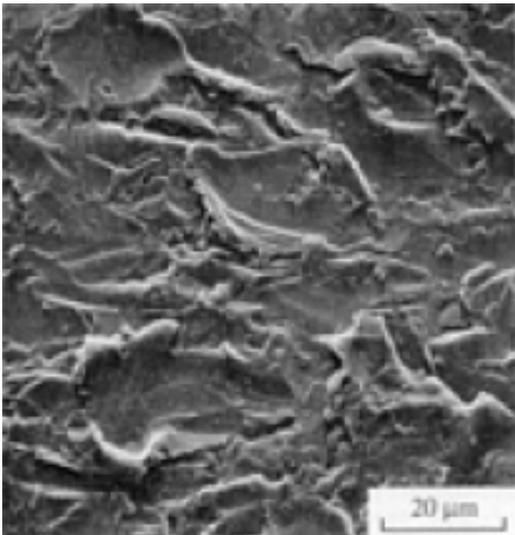
Figure 10. Surface of ductile commercial-purity nickel eroded by 130 μm Al_2O_3 at angle 20° and erodent velocity 53.8 m/s. Displaced "lips" of material are clearly visible at the ends of some impact creates [18]
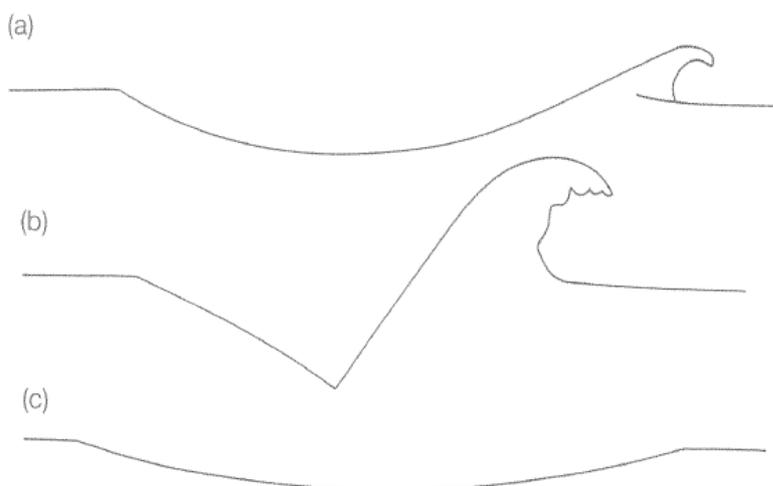
Figure 11. Types of wear of material depending on particles shape: a) ploughing deformation by spherical particles; b) cutting by angular particles rotating forwards; c) cutting by angular particles rotating backwards [19]
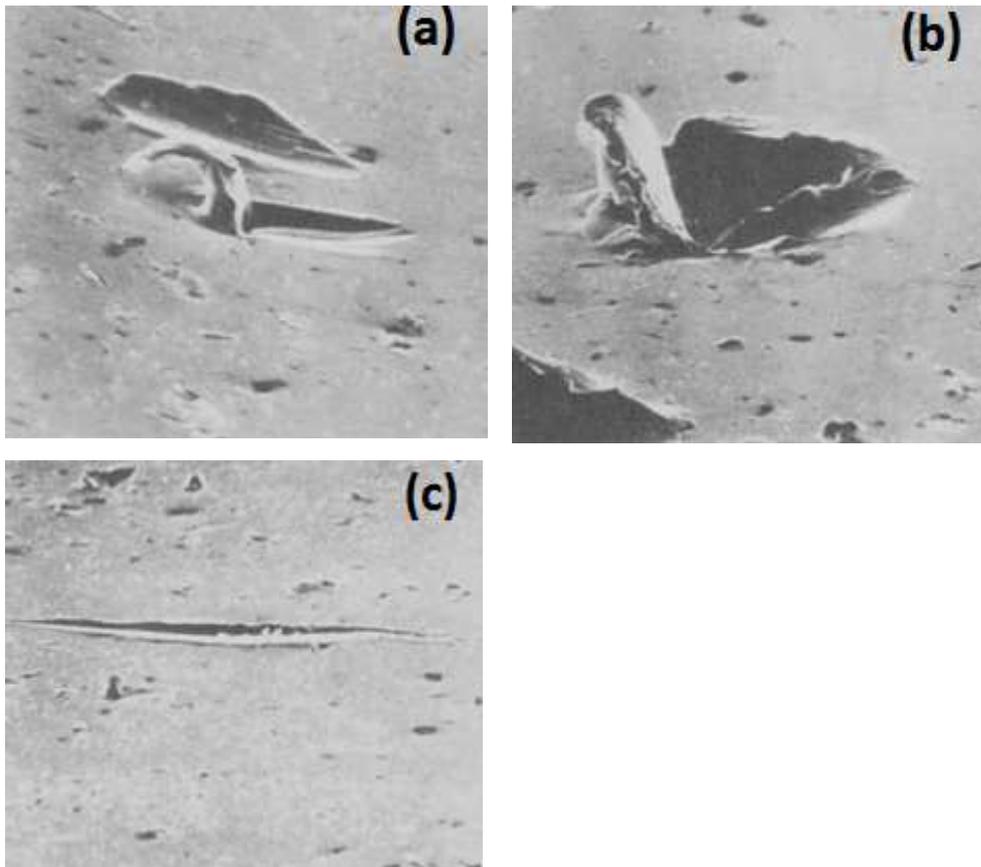
Figure 12. Types of wear of mild steel depending on particles shape. Quartz sand grains 420 – 500 μm, velocity 142 m/s, impact angle 25°. a) microcutting with formation of "lips" by spherical particles; b) deep cutting with removing of material to the end of the crater; c) microcutting [19]

2.4.3. Particle angularity parameters

The introduction of the computer-based image analysis systems has facilitated the use of numerical parameters in the description of particle shape. Typical shape parameters or shape factors, usually included in the image analysis software are the aspect ratio (width/length or sometimes length/width), roundness, form factor, convexity, elongation, etc. abrasive or erosive particles require numerical descriptors that include the measure of sharpness (or angularity) of particle protrusions. The first parameter developed that includes the sharpness of particle protrusions is called the spike parameter (SP). This descriptor is based on representing the particle boundary by a set of triangles constructed at different scales. The performance of the SP has been compared with more traditional shape parameters using artificially generated shapes (see Table 1) [20, 21].

Table 1. Artificial shapes with increasing angularity and the corresponding spike parameters, boundary fractal dimensions, roundness factors (perimeter^2/4π area) and aspect ratios (length/width). SP provides the angularity ranking of the computer-generated shapes that agrees well with the visual assessment of their abrasivity (the abrasivity increases from top to bottom) [22]

Shape	Spike parameter	Boundary fractal dimension	Roundness	Aspect ratio
●	0.1332	1.0046	1.1145	1.0000
●	0.1633	1.0064	1.1323	1.0078
●	0.1721	1.0063	1.2933	1.0556
●	0.1951	1.0115	1.1426	1.0514
●	0.2119	1.0095	1.6127	1.6800
✦	0.7243	1.0155	3.1458	1.0000

Disadvantage of this method is that at small scales it is sensitive to digitization errors, and this leads to some 'smooth' shapes being assigned an artificially high SP. For boundaries with convex shape and rounded protrusions, the apex angles of the triangles constructed at large scales are much smaller (sharper) than the corresponding protrusions. Also, since the method takes into account every boundary irregularity, the computing time can be long. Improved particle angularity parameter is the spike parameter quadratic (SPQ) fit. In this method, particle protrusions which are most likely to cause abrasion are isolated, while other boundary features are ignored. Only portions of a particle boundary, called spikes, protruding outside the circle of mean diameter, are considered in the calculation of the SPQ. The shape of the protrusions (spikes) is approximated by quadratic curves (see Figure 13). Relationship between erosive wear in air and the average SPQ parameter for different abrasive grits is shown in Figure 14 [22].
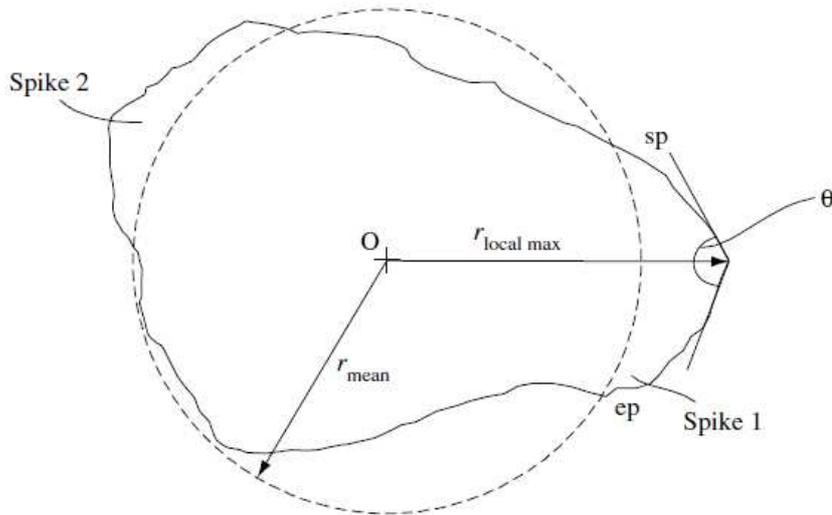
Figure 13. Method of the SPQ calculation by fitting quadratic segments to particle protrusions. For each spike, the local maximum radius is found and this point 'mp' is treated as the spike's apex. The sides of the spike, which are between the points 'sp-mp' and 'ep-mp', are then represented by fitting quadratic curves. Differentiating the curves at the 'mp' point yields the apex angle θ and the spike value sv = cos $\theta/2$. SPQ parameter is calculated as SPQ = SVaverage [23]
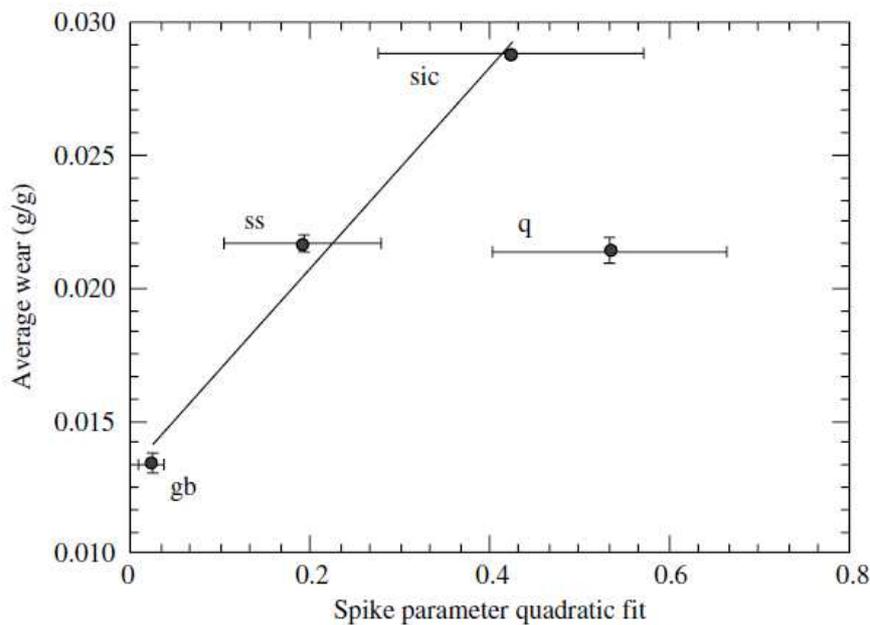
Figure 14. Relationship between erosive wear in air and the average SPQ parameter for different abrasive grits (gb – glass beads, ss – silica sand, g – garnet, d – natural industrial diamonds, sic – silicon carbide, q – crushed quartz and ca – crushed sintered alumina) at 90° impingement angle (error bars are ±1 standard deviation). The erosion rates are normalized with respect to density and particle velocity [24]

21

2.4.4. Particle size

The size of the particles usually ranges from 5 to 500 μm in size. Increasing particle size means enhanced impact energy. Hence brittle materials with a trend to cracking react more sensitively than ductile materials to changes of the particle sizes. Particle size not only affects the wear rate but generates the ranking of materials in terms of wear resistance (see Figure 15) The size of erodent particles has little or no effect on the erosion rate of ductile materials as long as the article size is above about 100 μm, but the erosion rate decreases rapidly with decreasing particle size below 100 μm [10, 25].

If the impinging particles are very small then only a minority of the impingement sites will coincide with a defect. The impingement site is a zone of highly stressed material directly beneath the particle on impact and similar in size to the particle. Plastic deformation is encouraged by an absence of defects and is the predominant mode of metal removal for small particles. Since repeated plastic deformation is required to remove material, this form of wear is relatively slow. Material removal by brittle processes is favoured by larger eroding particles. Since crack formation is rapid the brittle mode of erosion can be a very destructive form of wear [8].
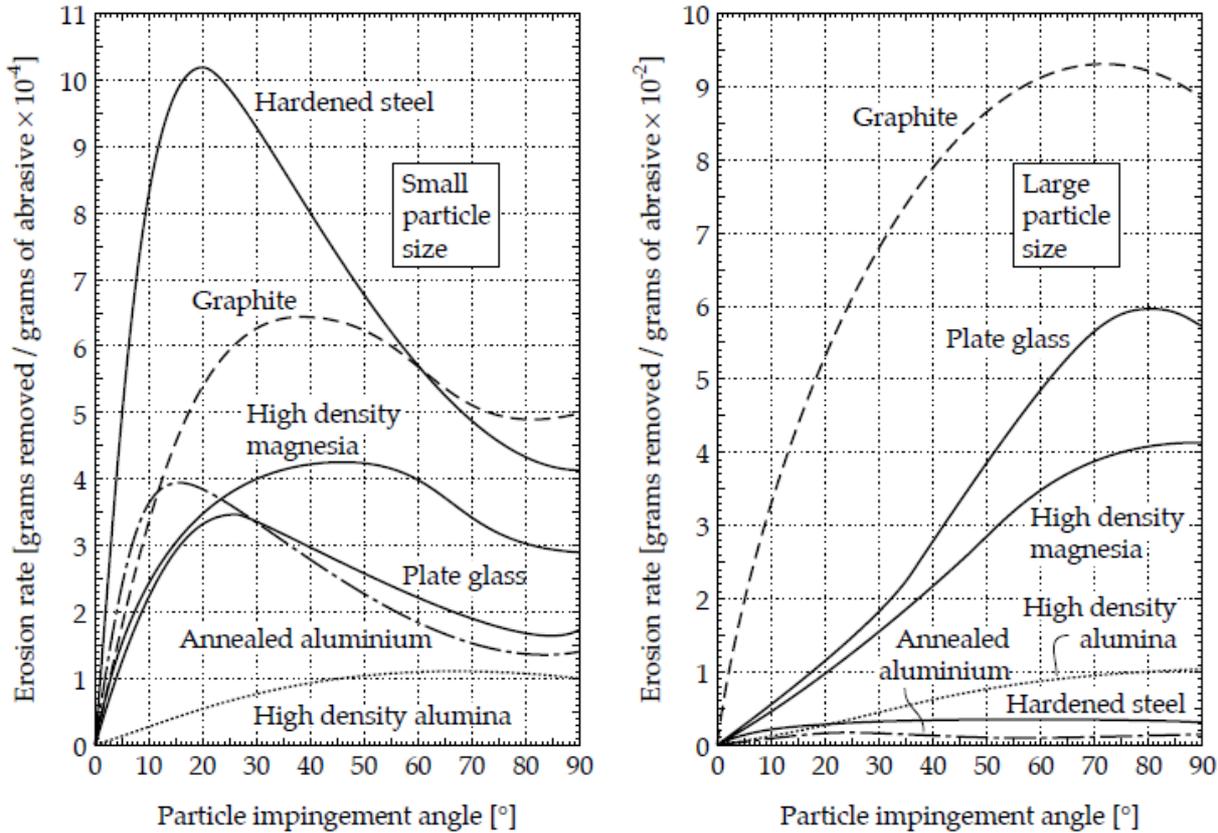
Figure 15. Effect of particle size on mode and rates of erosive wear. When the small particles were used as the erosive agent the materials ranked according to their wear resistance are in the following order: high density alumina > annealed aluminium > plate glass > high density magnesia > graphite and hardened steel. On the other hand, when the large particles were used as the erosive agent, the order changes to: annealed aluminium > hardened steel > high density alumina > high density magnesia > plate glass > graphite [26]

2.4.5. Angle of incidence

Impingement angles can range from 0° to 90°. At zero impingement angle there is negligible wear because the eroding particles do not impact the surface, although even at relatively small impingement angles of about 20°, severe wear may occur if the particles are hard and the surface is soft. A low angle of impingement favours wear processes similar to abrasion because the particles tend to track across the worn surface after impact. For ductile materials, such as plain carbon steels, maximum erosion rate is at low angles of incidence (typically 15° to 30°). For brittle materials, such as ceramics or hardened steel, erosion rate increases with increasing impact angles and have a maximum is at or near 90°. Erosion rates decrease continuously with increasing angles of impact for materials of very high elasticity such as rubber. The relationship between the wear rate and impact velocity for ductile and brittle materials is shown in Figure 16 [1, 27, 28].
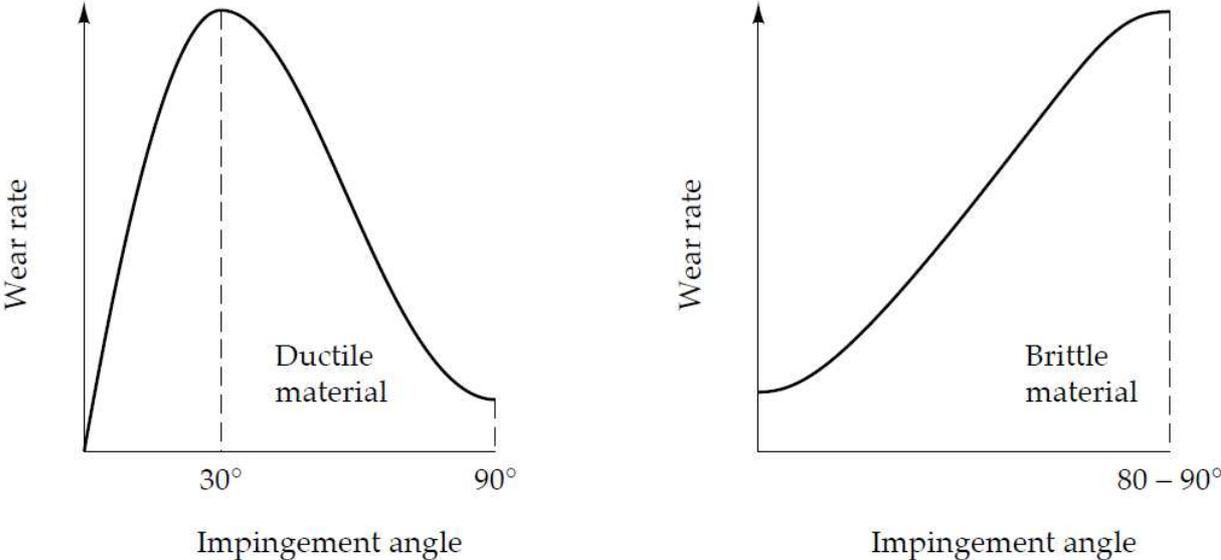
Figure 16. Scheme of erosion rate as function of impingement angle [8]

23

2.4.6. Particle flux

Flux rate of the particle, or the mass of impacting material per unit area and time is another controlling parameter of erosive wear rates. Erosive wear rate is proportional to the flux rate up to a certain limiting value of wear. The limiting particle flux rate is highly variable, ranging from as low as 100 kg/m²s for elastomers to as high as 10,000 kg/m²s for erosion against metals by large and fast particles. Increasing of flux interference of rebounding particles with incident particles, leads to protection of surface - the result being that erosion rate decreases exponentially with increasing flux. The effect increases with decreasing velocity or particle size and depends on material through the effect of rebound velocity, which affects the time during which the rebounding particles shield the surface [29, 30].

2.4.7. Embedding of erodent fragments

The influence of embedding of fragments of the erosive particles in the specimen surface is in some cases considerable. By testing Al_2O_3 erosion of copper and for Al_2O_3 erosion of nickel it is clearly understandable that normal-incidence erosion produce a continuous composite surface layer, consisting of particle fragments mixed with the eroded metal, which is actually self supporting when the underlying substrate is electropolished away. Observation by transmission electron microscopy show that the Al_2O_3 particle size presents only in the layer of 0.1 μm, compared with 23 μm size of incident particles, indicating that embedded fragments are subsequently refragmented by further impacts. 100-grit Al_2O_3 produce a discontinuous composite layer at normal incidence and 53 m/s [9, 19, 31].

2.4.8. Surface hardness

Hardness, work hardening and the capability of deformation are important physical properties of the target metal for its resistance to wear. Dynamic hardness and work hardening of the target determine the amount of plastic deformation and hence the depth of impact craters at a given impact energy and angle of incidence. Capability of deformation of the metal during impact loading affects the number of impacts which are required for the formation of wear debris. As a result, a softer metal can show greater erosion resistance than a harder one [13, 32].

2.4.9. Particle hardness

Hard particles cause higher wear rates than soft particles. The effect of particle hardness on wear depends on the particular mode of erosive wear taking place, e.g. ductile or brittle. In the brittle mode the effect of particle hardness is much more pronounced than in the ductile mode. Particle will indent the surface if particle hardness H_a is greater than ~1.2 times the surface hardness H_s (see Figure 17). If H_a is less than ~1.2 H_s, plastic flow will occur in the particle, which will be blunted [10].

Figure 17. a) H_a> 1,2 H_s; b) H_a< 1,2 H_s [10]

2.4.10. Erosion media

In practice, erosion is always accompanied by medium, water or air. In case of solid particle erosion air flow may be considered as medium. The effect of the medium is to alter the trajectory, speed, impingement angle and even to cause wear. Turbulence of the medium accelerates erosive wear as particle impingement is more likely to occur in turbulent flow than in laminar flow where the medium tends to draw the particles parallel to the surface. That helps to predict particles trajectory. The difference between the particle behaviour in laminar and turbulent flow of the medium is illustrated in Figure 18. An exception to this rule is where the laminar flow is directed normally to the surface which is the case when a jet of fluid impinges against a surface. In this case, wear is concentrated directly beneath the jet and a relatively unworn annular area surrounds the wear scar. This phenomenon is known as the 'halo effect'. The effect of increasing turbulence with distance from the jet is outweighed by the concentration of erosion directly beneath the jet [33, 34, 35].
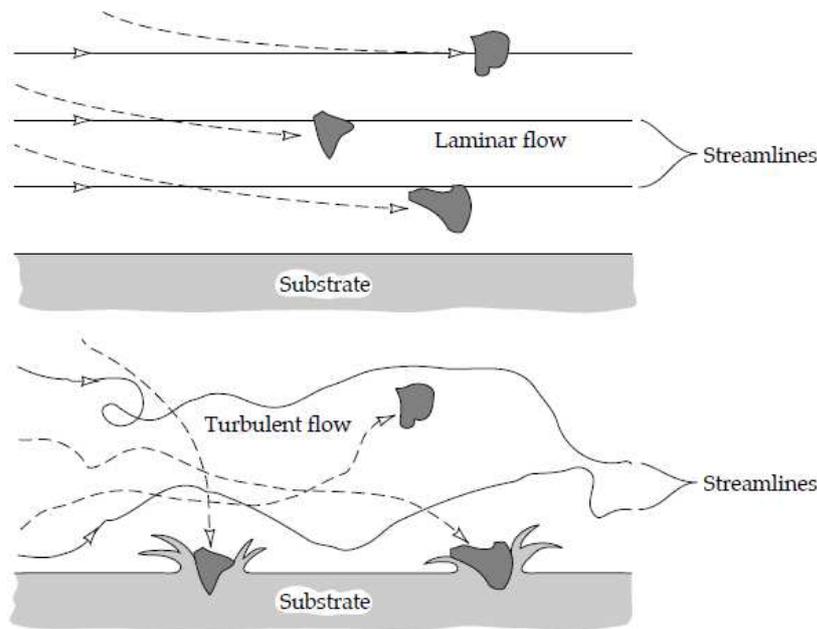
Figure 18. Effect of flow on erosive wear [8]

2.4.11. Temperature

The rate and mechanism of erosive wear are influenced by temperature. The primary effect of temperature is to soften the eroded material and increase wear rates. It is not having sufficient effect until temperatures higher than 600 °C are reached and the erosion rate shows significant increase. This temperature coincides with the softening point of the steel. When high temperature erosion of metals occurs in an oxidizing medium, corrosion can take place and further accelerate wear. Material is removed from the eroding surface as a relatively brittle oxide and this process of wear can be far more rapid than the erosion of ductile metal. The underlying metal does not come into contact with the impinging particles at sufficiently high temperatures because of the thick oxide layer present and then oxidation rates control the erosive wear. The relationship between the erosion rate and temperature is shown in Figure 19 [13].
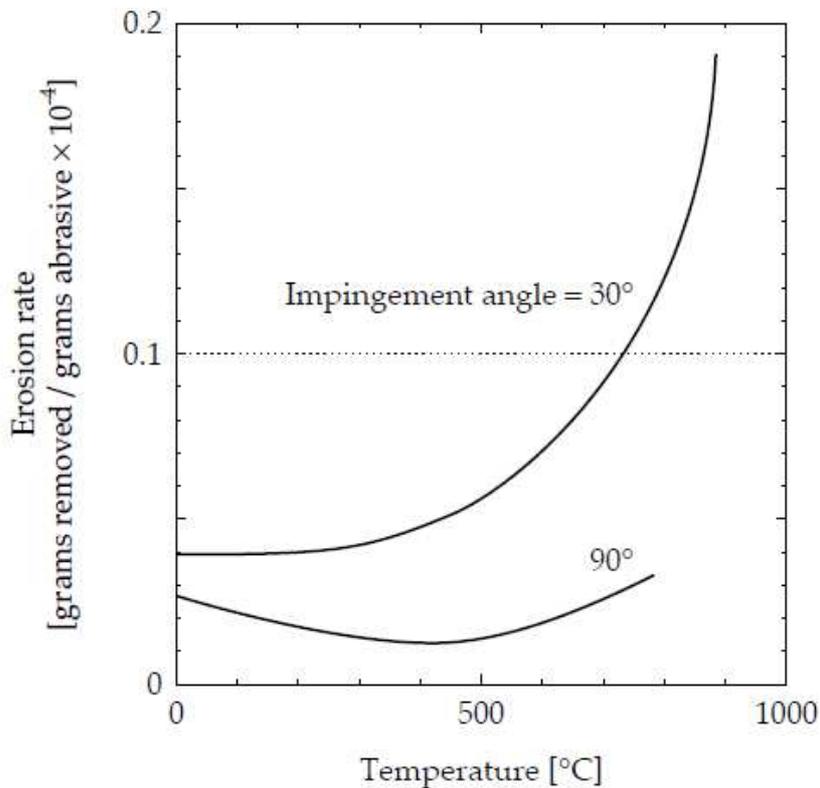
Figure 19. Scheme of erosion rate as function of temperature [38]

2.5. Erosion – corrosion mechanism

In practice almost neither erosion or corrosion can exist without each over. For better understanding erosion/corrosion can be separated into two regimes - dominated by erosion or corrosion, depending on which process occurs at the greater rate under the conditions of interest. For very low corrosion rates and/or highly erosive conditions, erosion dominates and basically pure erosion is expected. For high corrosion rates or mild erosion conditions, corrosion dominates. Between these extremes, important synergistic interactions can increase the wear rate significantly beyond that due to either erosion or corrosion alone. If corrosion take place, synergetic process between pure erosion and pure corrosion can be divided into two separate categories: erosion-enhanced corrosion and corrosion-affected erosion. Pure erosion occurs when the corrosion rate is negligible compared with the erosion rate, as in severe erosion conditions (high-velocity, angular particles) or in non-corroding conditions such as an inert gas. In a corrosive gas, this regime would be confined to relatively low temperatures [39, 40].

2.5.2. Corrosion - affected erosion

In the presence of corrosion-affected erosion the damage zone includes both scale and metal. Corrosion-affected erosion can be characterized with an increased corrosion component, a thin composite scale on surface is developed, but the dimensions of the stress field introduced by the embedded erodent particles are greater than the scale thickness, so that both scale and metal are deformed. The metal loss rate is increased over that for pure erosion, and a surface composite of metal, scale, and erodent particle fragments is typically produced [41].

2.5.3. Erosion-enhanced corrosion

The main point of that is the dimension of the impact damage zone is confined within a thick scale. Erosion-enhanced corrosion causes increased metal thickness loss rates because erosion reduces the scale thickness and therefore increases the corrosion rate, which is controlled by transport of metal or corrosive elements (oxygen, sulphur). Scale spallation can also be involved.

Erosion-enhanced corrosion consists of three categories. First step involves spalling of the scale. Second and third are determined by the relative erosion and corrosion rates, involve a steady-state scale thickness. Metals likely to be of use in high-temperature applications in air or other corrosive atmospheres are those that form protective scales that grow naturally in a state of compression, because the volume of scale formed from a given amount of metal exceeds that of the metal consumed. The compressive stress combats fracture, resulting in a protective scale free of cracks and pores. Scales that form in tension generally crack and are non-protective. After a short initial stage, protective scale growth is limited by the diffusion of either metal outward or of the oxidant (oxygen, sulphur, halogen) inward through the scale thickness. Scheme of erosion-corrosion mechanism is shown in Figure 20 [42, 43].
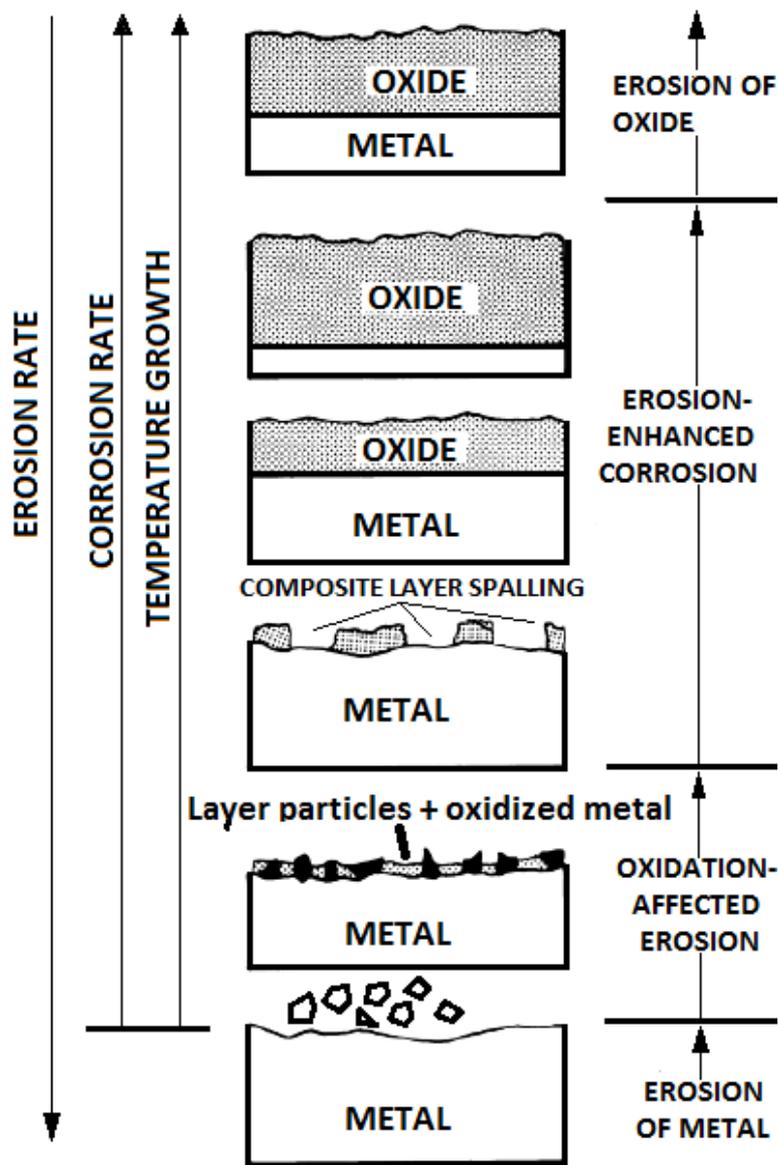
Figure 20. Erosion / Corrosion mechanism [44]

2.6. Comparison between abrasive and erosive wear

In different situations, erosion is very similar to abrasion and the boundary between these two phenomena must be clarified. Particularly for very dense particle distributions in liquid or gas media, in which a "pack" of particles can develop and slide across the surface. It should be clarified that solid particle erosion refers to a series of particles striking and rebounding from the surface, while abrasion results from the sliding of abrasive particles across a surface under the action of an externally applied force. The clearest distinction is that, in erosion, the

force exerted by the particles on the material is due to their deceleration, while in abrasion it is externally applied and approximately constant [1].

Table 2. Similarities and differences between abrasion and solid particle erosion [5, 13, 22, 45]

Comparative parameters	Abrasion	Solid particle erosion
Wear by brittle fracture	identical mechanisms of cracking: formation of median and lateral cracks	
Wear by plastic deformation	identical mechanisms of microcutting or microploughing	
Number of solids in process	two-body, three-body	surface and particle
Size of particles or grits	without limits	commonly 5 - 500 μm
Speed of particles or bodies	without limits	commonly 15 - 170 m/s
Movement type of particles	sliding with externally applied force	striking and rebounding
Media	can be gaseous or fluid	

2.7. Structural ceramics

Ceramic materials can be classified as: advanced structural ceramics, electronic ceramics and optical ceramics. In tribology ceramics are usually presented by structural ceramics due to their unique properties as tribomaterials that include resistance to wear and corrosion at elevated temperatures, low density, and unique electrical, thermal, and magnetic properties. Structural ceramics can be classified into two classes: oxide ceramics (Al_2O_3, ZrO_2, SiO_2, etc.) and non-oxide ceramics (SiC, TiC, TiB_2, Si_3N_4, TiN, etc.) [46, 47].

2.7.1. Properties

Ceramics can be characterized as brittle materials that can contain pores. They differ from metal alloys in that they are ionic or covalent bonded crystals. The bonds between atoms in covalently bonded ceramic materials are very strong and highly directional. Thus bonds are highly stable and the result is high melting points. Ceramics are generally used at high

temperatures (more than 1000 °C), or in situations where frictional heating generates high surface temperatures, where any other material class cannot be used. As far as maximum operating temperature is concerned, nickel based superalloys are typically used at 1000 °C, while some nitride and some oxide ceramics can be used at temperatures close to 1500 °C. In terms of elastic modulus or hardness, ceramics are much better than refractory metals. Hardness of Al_2O_3 is around 19 GPa, which is close to 3 times the hardness value of fully hardened martensitic steel (~7 GPa). Ceramics such as TiB_2, have hardness of around 28 GPa. Elastic modulus of Al_2O_3 is around 390 GPa, which is close to double that of some steels (210 GPa). The higher elastic modulus of ceramics provides them with good resistance to contact damage. Ceramics can be toughened by modifying the structure with small amounts of additives. Toughening can be achieved by the development of beneficial residual stresses. For example alumina can be toughened by 10 % to 20 % of zirconia (ZTA). Addition of zirconia increase strength and elastic modulus plus two to three fold increase in fracture toughness without an increase in density [48, 49]. Properties of structural ceramics are schematically presented in Figure 21.
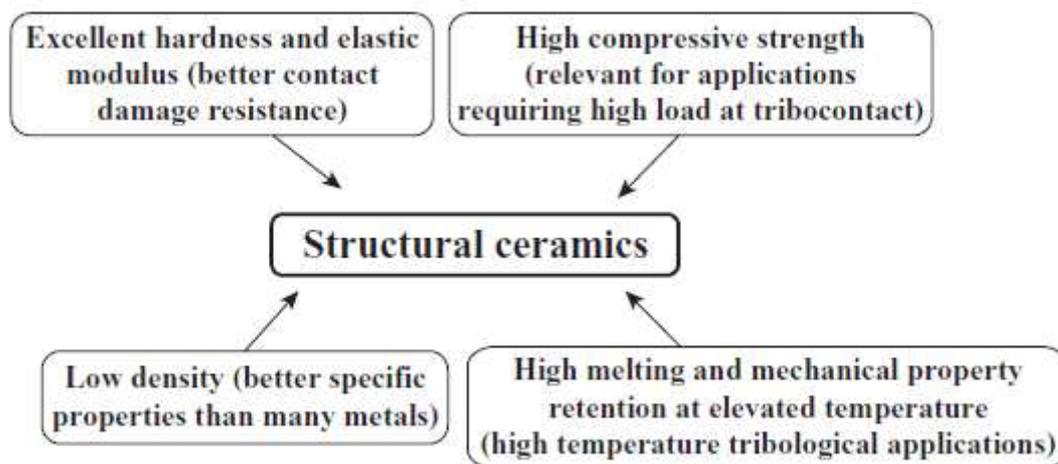
Figure 21. Various properties of relevance to tribological applications of structural ceramics [48]

2.7.2. Wear properties

Ceramics are sensitive to high contact stresses or to any contact condition leading to a state of stress that contains tensile components and inclined to respond to stress by brittle fracture. That leads to crack formation on surface or subsurface. Brittle fracture of ceramics due to

concentrated contact can be understood in terms of Hertz elastic stress distribution. Crack growth also is sensitive to environmental influences. For example presence of water increases the crack growth rate dramatically in alumina [10].

Ceramics can deform plastically under the hydrostatic stress associated with concentrated contacts, but the plastic deformation is very small, when compared with metals and polymers. Increasing the temperature of a ceramic material to about 0.6 times below the melting point, increases the potential for plastic deformation. Strength reduction and increased creep rates assist in the rising of temperature. However, the increase in plasticity with increase in temperature does not produce the ductility that is common in metals and persists a brittle or semi-brittle behaviour. The thermal-shock-induced fracture of ceramics is a serious wear problem. Large thermal gradients can develop in ceramics during frictional heating, because of low thermal conductivity. When quenched, these hot spots develop large tensile stresses and cracks develop. The result is an increase in wear as relatively large pieces break out of the surface. These processes can cause a failure by fracture. Ceramics are sensitive to strain rate and will exhibit an increased tendency to cracking with increased sliding velocity, in addition to the frictional heating. Sensitivity to impact makes ceramics vulnerable to erosive wear. Ceramics show high erosive wear when the erosive particle angle is close to 90°. The relative hardness of the ceramic and eroding particles is important to erosion mechanisms of ceramics. Ceramic will resist particle erosion as long as the eroding particle is much softer than ceramic material. If the particle is harder than the ceramic, then the erosion rate can be minimized by providing as much toughness as possible, a small grain size, and minimum porosity. When the particle is either softer or about as hard as the ceramic, a small increase in its hardness causes a large increase in erosive wear. When the particle is much harder than the ceramic, microstructure and fracture toughness become more important to resist erosion [5, 50, 51].

2.7.3. Applications

Due to wear properties structural ceramics are used in many mechanisms which are involved in structural or tribological applications (see examples in Figure 22). This part will shortly overview most of it (Table 3).

Table 3. Applications of structural ceramics [52, 53]

Type of application	Type of structural ceramics
Valve balls	Silicon nitride
Rollers in furnace conveyors	Silicon nitride
Piston rings in low heat loss	Silicon nitride
Ball bearings in high-temperature heat engines	Silicon nitride
Medical prostheses	Alumina
Computer tape guides and capstans	Alumina
Wear plates in coal slurry pumping systems	Alumina
Cylinder liners and valve seats in low heat loss diesel engines	Zirconia
Cutting tools	Silicon nitride, Alumina, Sialon
Face seals, floating ring seals	Silicon carbide, Alumina
Ceramic dies	Alumina, Zirconia, Sialon
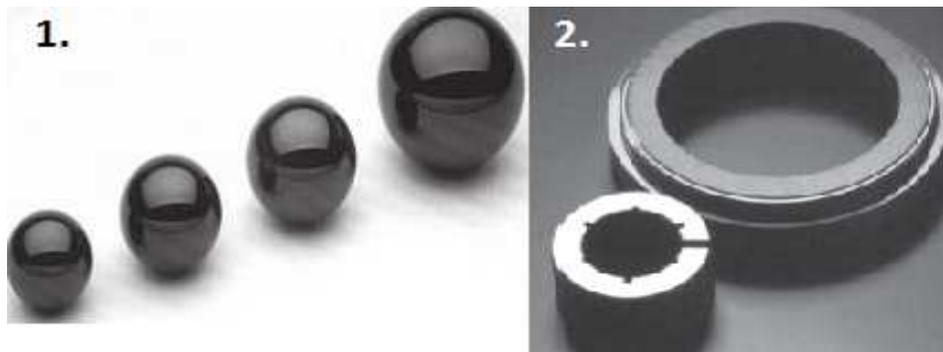
Figure 22. Example of structural ceramics: 1) silicon nitride check valve balls from around 20 mm to around 40 mm in diameter; 2) silicon carbide seals [46]

2.8. Erosive wear resistance of materials

There is no general criteria to define, if material is erosion resistive or not. Each group of material should be considered separately to define it, because of different characteristics of materials have particular protection mechanism to avoid high erosion rates. There are two different erosive wear protection mechanisms that can take place, achieved by more than one type of material. In some cases the material can be extremely hard and tough so that the impacting particle is unable to make any impression on the surface (see Figure 23). This is the approach adapted when developing metallic or ceramic erosion resistant materials. On the other hand, the material can be tough but with an extremely low elastic modulus so that the kinetic energy of the particles is harmlessly dissipated [54].
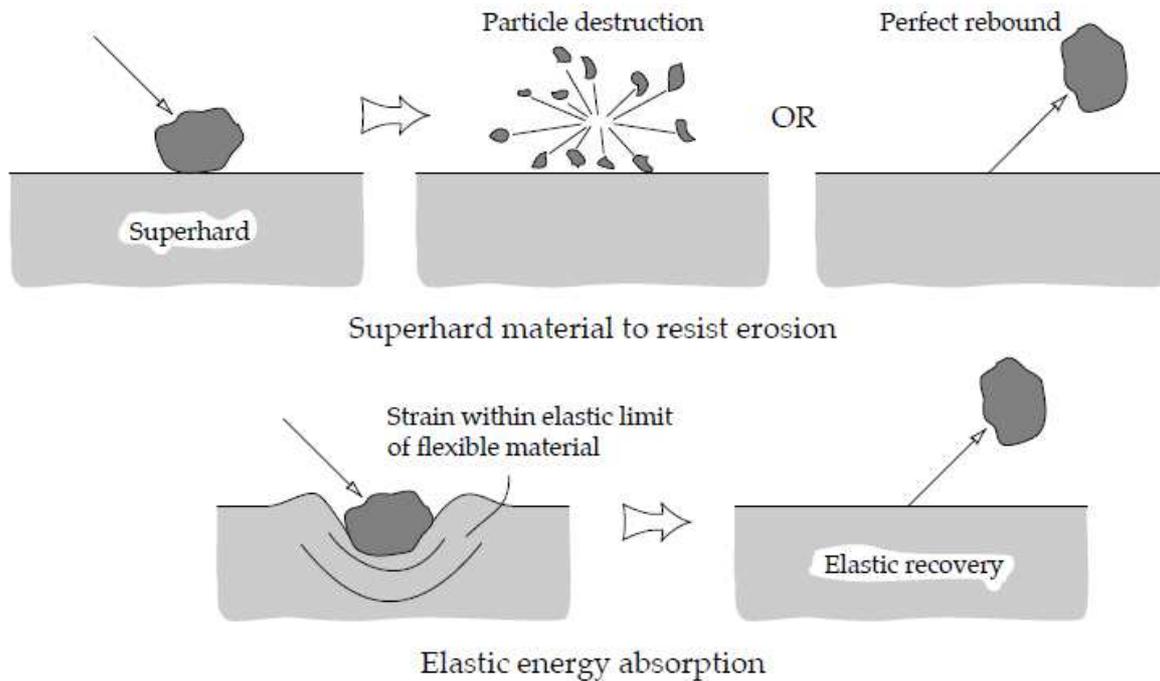
Figure 23. Mechanisms of materials to avoid erosion [54]

Heat treatment of steel to increase hardness improves erosive wear resistance at low impact angles but lessens the erosive wear resistance at high impact angles. There are PH-55A series of stainless steels containing molybdenum which can be precipitation hardened. These alloys have been developed to provide combined corrosion, abrasion and erosion resistance. They also will resist excessive oxidation at elevated temperature [55, 56].

Polymethylmethacrylate is used for aircraft windscreens as resistant material to high speed erosion by sand, dust and rain. Reinforced polymers such as chopped graphite fibre in a thermoplastic polyphenylene sulphide (PPS), woven aramid fibre in reinforced epoxy laminate (Kevlar 49/epoxy) also have low erosive wear rates [57, 58].

Rubber is a good erosive wear resistive material. Due to the elasticity of rubber, impingement of particles on a rubber surface produces elastic deformation only and, therefore, the eroding particles bounce off harmlessly. If the particles are sharp and attack at a low angle, cutting wear will result. Thus, the higher impingement angle is to the surface, the less likely will rubber wear by erosion [59, 60].

Structural ceramics are used in diverse tribological applications (precision instrument bearings, cutting tool inserts, prosthetic artificial joints, engine components) due to their unique properties that include resistance to abrasion and erosion at elevated temperatures. Oxide ceramics such as alumina, zirconia and zirconia toughened alumina appear to have the

higher erosive wear resistance. A silicon carbide fibre - silicon carbide matrix composite was found to have a higher erosive wear rate than chromium alloy steel at 25°C, but considerably less than the same steel at 850°C . Cermets consisting of tungsten carbide grains in a cobalt binder matrix are also used for erosive wear resistance [61, 62, 63].

Different coatings can be used to decrease erosion rate of materials. Chemical vapor deposition with SiC is an excellent coating material where resistance to wear, erosion or oxidation is required. Diamond-like carbon films can be used where resistance to erosion, abrasion or adhesion is needed. Applications for diamond coatings: mechanical seals, sliding bearings, wire-drawing dies, high-precision microdrills, surgical blades, jet nozzles [64].

3. PRACTICAL PART

A test has been performed in order to make an assessment of behaviour of castable ceramics reinforced by various additives and to determine the effect of their concentrations in erosive conditions at different temperature. Production of such low cost castable ceramic compositions with high erosive wear resistance, can be useful in production of supporting and/or protective elements working at room and high temperature. To decrease brittleness and improve such ceramic material mechanical properties like compressive, flexural and tensile strength, such reinforcement agents like basalt fibers, particles and flakes are used in ceramic material production [65]. Due to their ceramic nature and low price, basalt fibers are good reinforcement agents in various types of matrices (e.g. polymer, concrete, metallic, etc) [66]. To estimate the influence of temperature on wear properties of obtained composites, it was decided to test samples in three different temperature regimes.

3.1. Materials of specimens

3.1.1. Liquid glass

Liquid glass is a water solution of soluble glass consisting of sodium or potassium silicate. Under the influence of air or carbon dioxide begins hardening of liquid glass. Hardening of liquid glass takes a long period of time due to occurring on surface layers thin film that prevent liquid glass from CO_2 and drying out. To fasten the process of hardening it is

necessary to use catalysts, mainly silica sodium fluoride (Na_2SiF_6). Reaction of generating dissoluble gel of silica acid that hardens and connects together grains of filler and proceeds quickly (within 10-15 minutes) begins after adding catalyst to liquid glass [67]:

$$Na_2 SiF_6 + 2 Na_2SiO_3 + 6 H_2O = 6 NaF + 3 Si(OH)_4$$

Wide range of fireproof coatings is based on liquid glass. Liquid glass is available and has a good thermal resistance that makes it perspective in designing coatings with high durability in case of low density (200 – 300 kg/m^3). Moreover, this coating has good adhesion to other materials. In material development with a component like liquid glass may appear problems due to moisture of liquid glass. It contains about 50 wt.% - 60 wt.% of water, that leads to porous and coarse-grained structure of material after process of heating and removing water. To avoid this phenomenon, all "free" water (removable at temperature up to 105 °C) should be removed and strongly combined water (removable at temperature above 110 °C) should be kept [67, 68].

According to available recommendations for acid resistant composition production based on liquid glass and high temperature resistive basalt powder new recipes was proposed for castable ceramic by using liquid glass (sodium metasilicate, Na_2SiO_3 from Keemia Kaubandus) with hardening accelerator (sodium hexafuorosilicate, Na_2SiF_6 from Alfa Aesar). Additionally the sand (U.S Silica Company, Ottawa, particle sizes of 0,2 to 0,3 mm) was added in this investigation to understand influence of relative large size of particles on wear behaviour of samples and compare results to more expensive crystalline silica flour [69, 70, 71, 72].

3.1.2. Basalt

Adding of basalt "scale" into a structure of liquid glass material is increasing its strength, because of dispersion reinforcement and generating of uniform structure. As a result of using liquid glass with effective filling materials like basalt, it is possible to design materials with unique combination of characteristics: low factor of thermal conductivity, uninflammable, ecological, with low cost [68].

Different concentrations of basalt as reinforcement material were used in combination with castable ceramics R750. As reinforcement additivities were used basalt powder (made by using disintegrator, particle sizes of 0-25 μm), basalt fibers from company Kamenny Vek

Ltd. (see Table 4), activated basalt flakes from company Otselot, (see Table 5) were used [73, 74].

Table 4. Physical properties of used basalt fibers [22]

Property	Description
Monofilament diameter	13 µm
Cut length	3,2 mm

Table 5. Physical properties of used basalt flakes [23]

Average size of flakes	0,25x3 mm
Thickness	1 – 4 µm
Moisture content	< 0,5 – 0,6%

3.1.3. Rescor castable ceramics

Cotronics corporation offers a variety of castable ceramics like alumina, silicon carbide, zirconium oxide, fused silica, insulating ceramic foam. This ceramics have a good resistance to high temperature (up to 2200° C), thermal shock, molten metals, oxidizing, reducing atmospheres, acids and alkalis. Rescor castable ceramics can satisfy many advanced requirements for "in house" fabrication of high strength parts and prototypes and they are good solution for production, research and development applications. Characteristics of ceramics that were chosen for testing are given in Table 6. For obtaining castable mass, liquid activators (made by Cotronics Corp) adapted for each base: Rescor 750 Activator (R750A), Rescor 780 Activator (R780A) and Rescor 760 Activator (R760A) have been used [75].

Table 6. Characteristics of castable ceramics, used in test [75]

Designation	750	760	780
Base	SiO₂	ZrO₂	Al₂O₃
	Fused silica	Zirconium oxide	Alumina oxide
Color	white	tan	white
Possible shapes			
Compressive strength, [MPa]	41	28	41
Modulus of rupture, [MPa]	10	8	12
Thermal conductivity, [W/(cm·°C)]	0.0058	0.0093	0.0144
Max. Temperature, [°C]	1480	2200	1650
Moisture resistance	Excellent	Excellent	Excellent

3.1.4 Silica sand

Silica sand Microsil M4 produced by Sibelco Group has been used as reinforcement material. A selected silica sand with a SiO_2 content of over 99 % is produced by iron free grinding and accurate sieving by means of air- separators used in ceramics, tile-glues, special mortars, coatings [21].

3.2. Equipment

High temperature centrifugal erosion tester CAK–HET (similar to GOST 23.201-78.1978), produced in Tallinn University of Technology to determine the effect of testing conditions on erosion rate of materials at high temperatures (up to 700 °C). Accelerator uses circular motion to generate a continuous stream of particles. It is schematically presented in Figure 24. The erodent particles are fed into the centre of the rotor, and move outwards along radial channels, leaving the rotor at a speed governed by the peripheral speed of the rotor. The strength of fastening should be enough to fasten specimen during experiment but not too high to brake it since ceramics are materials that are brittle enough and have low bending strength. Equipment has one disadvantage connected with heating elements. Heating springs can deform and have problems with connections due to their vertical position and long-term high temperature tests. To solve this problem it was proposed to change arrangement of spirals from vertical to horizontal and select suitable material for supports that will be resistant to high temperature erosion. This technology will be used in new erosion tester (see Figure 25). Experimental materials, created and tested in this work
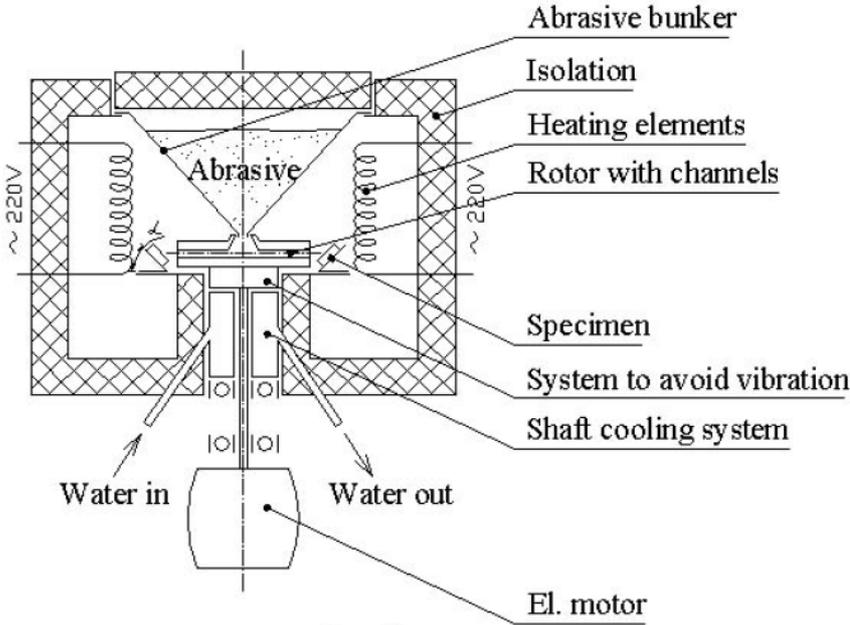
Figure 24. Scheme of erosion tester [78]
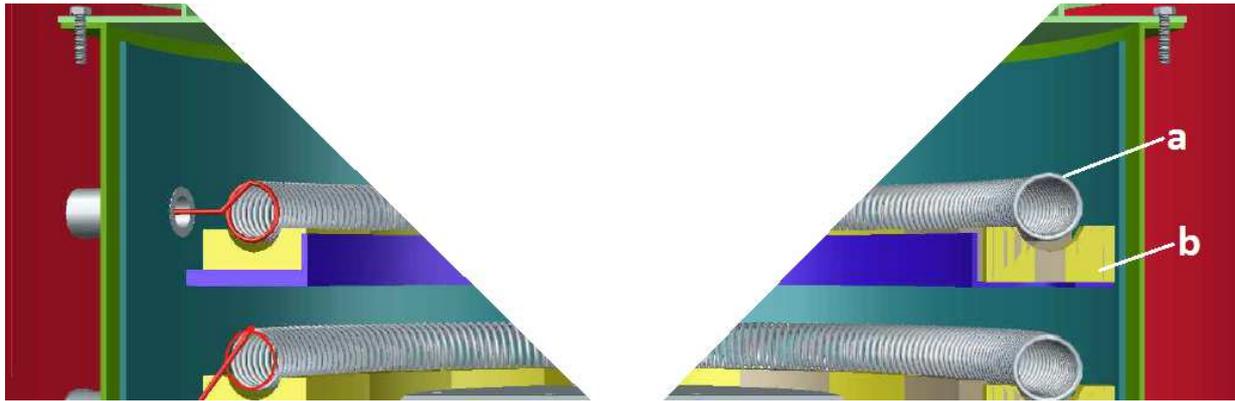
Figure 25. Scheme of construction of new erosion tester with horizontal heating springs (a) and ceramic supports (b) (shown partially, drawing made by Janis Baroninš)

For thermal processing was used the new muffle furnace Nabertherm model L9/13 (see Figure 26) purchased by Tallinn University of Technology for laboratory tests was used for thermal processing. Heating elements on support tubes are radiating freely into the furnace chamber and provide particularly short heating times for these models. Thanks to their robust lightweight refractory brick insulation, they can reach a maximum working temperature of 1300 °C [79].

Figure 26. Muffle furnace Nabertherm L9/13 [79]

3.3. Specimen`s installation method

Stationary specimens are arranged around the rotor. Maximum amount of specimens is twenty. Possible impact angles (α) are 30°, 45°, 60°, 75° and 90°. Specimen is mounted to support with special bracket and wedge. To reach faster and easier way of specimen installation, there was introduced new type of wedge, which also provides stable position during testing. Wooden wedge was used for test at room temperature. For tests at elevated temperatures two metal wedges were used: thick and thin. Thin wedge was produced from

thin piece of stainless steel. It works like a spring and gently presses specimen to bracket with force that is low but sufficient to fasten the specimen. The wedge is installed by hammer slowly and with a slight force to avoid cracking of specimens. Method of installation of specimens is illustrated in Figure 27 and in Figure 28.

Figure 27. Fixed specimens on the rim of rotor for test at room temperature
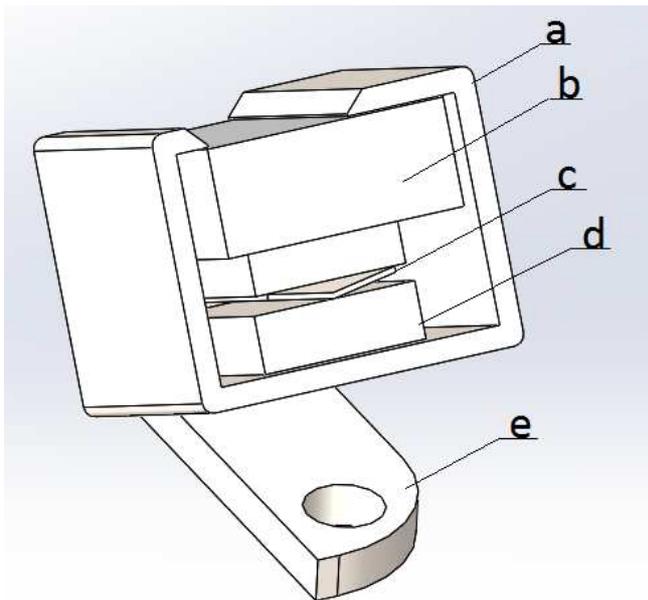
Figure 28. Specimen installed in bracket with new type of wedge. a) bracket; b) specimen; c) metal spring wedge; d) metal wedge (if required); e) holder

3.4. Technology of fabrication of specimens

Method of producing specimens 1 – 14

- mixing powders in a rapid laboratory rotating mixer (blender type)

- adding activator

- mixing by the special glass stick in a plastic can

- placing of prepared mixture into a silicon form and mixing

- vibrating on the special vibration table for 2 to 5 minutes

- first drying at room temperature

- specimen demolding

- second drying in the furnace at 120 ℃

- thermal processing in the furnace at 950 ℃, starting temperature 120 ℃, instantly after second drying

- cooling down in the furnace to room temperature

Mineral compositions of samples (1 – 14) are listed in Table 7.

Table 7. Mineral compositions for specimens

Specimen No.	Base, wt%	Activator, wt%	Reinforcement, wt%
1	Rescor 750, 78%	22%	-
2	Rescor 750, 69%	24%	Basalt powder, 7%
3	Rescor 750, 59%	22%	Basalt powder, 19%
4	Rescor 750, 69%	26%	Basalt fibers, 5%
5	Rescor 750, 75%	24%	Basalt fibers, 1%
6	Rescor 750, 58%	31%	Basalt fibers, 11%
7	Rescor 750, 67%	22%	Microsil M4, 11%
8	Rescor 750, 50%	22%	Microsil M4, 28%
9	Rescor 750, 40%	22%	Microsil M4, 38%
10	Rescor 750, 76%	22%	Basalt flakes, 2%
11	Rescor 750, 69%	25%	Basalt flakes, 6%
12	Rescor 750, 59%	29%	Basalt flakes, 12%
13	Rescor 780, 78%	22%	-
14	Rescor 760, 78%	22%	-

Method of producing specimens 15-18

- mixing powders in a rapid laboratory rotating mixer

- adding liquid glass

- mixing by the special glass stick in a plastic can

- placing of prepared mixture into a silicon form and mixing

- vibrating on the special vibration table for 2 to 5 minutes

- first drying at room temperature

- specimen demolding

- specimen drying in an oven (Nabertherm L9/B equipped with P330 controller) at 90 °C (with heating from 25 °C, 5°C/min)

- cooling down after drying in the furnace with the open door

Mineral compositions of samples (15 – 18) are listed in Table 8.

Table 8. Mineral composition for new design composites based on liquid glass

Specimen No.	Base, wt%	Activator, wt%	Reinforcement, wt%
15	Liquid glass, 22%	2%	Basalt powder, 65%
16	Liquid glass, 22%	2%	Basalt flakes, 65%
17	Liquid glass, 22%	2%	Microsil M4, 65%
18	Liquid glass, 22%	2%	Sand, 65%

3.5. Operations during the testing procedure

1. marking specimens with diamond mill, that was mounted on Dremel 3000 (Figure 29)

Figure 29. Dremel 3000 – rotary multitool with changing nozzles [80]

2. cleaning by compressed air, because cleaning with liquid is not possible due to porous nature of samples

3. weighing of specimens

4. installing specimens into the special holders

5. installing of ring with holders into the equipment for erosion testing

6. choosing frequency of rotation and temperature (before each test)

7. erosion test at room temperature (phase 1)

8. taking off specimens after the end of the test, cleaning, weighing, installing of same samples

9. erosion test at 300 ℃ (phase 2)

10. slow cooling down to 100 ℃ during 2 hours, to reduce cracking due to thermal stresses

11. taking off specimens after the end of the test, cleaning, weighing, installing of same samples

12. erosion test at 600 ℃ (phase 3)

13. slow cooling down to 150 ℃ during 4 hours, to reduce cracking due to thermal stresses

14. taking off specimens after the end of the test, cleaning, weighing

Testing has been made in three phases in different conditions with the same specimens. Test conditions are shown in Table 9. However, it should be noted that due to brittleness of specimens only nineteen of twenty had continued the third phase, also specimens 4 and 14,

had lost about 50% of mass during installation. Micrographs of all specimens after third phase are shown below (Figures 30-48).

Table 9. Test conditions

	Temperature, °C	Velocity, m/s	Angle of erosion, º	Mass of particles, kg (Estonian sand: Batch IV)
First phase	20	20	30	6
Second phase	300	20	30	6
Third phase	600	20	30	6

Figure 30. Specimen No.1 after test at 600 °C , commercial ceramics Rescor 750 based on SiO_2
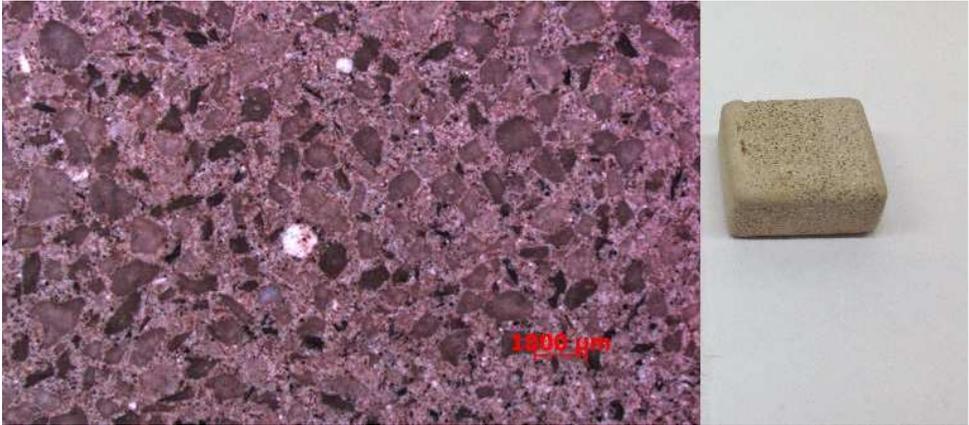
Figure 31. Specimen No.2 after test at 600 °C, commercial ceramics Rescor 750 reinforced with 7 wt.% of basalt powder
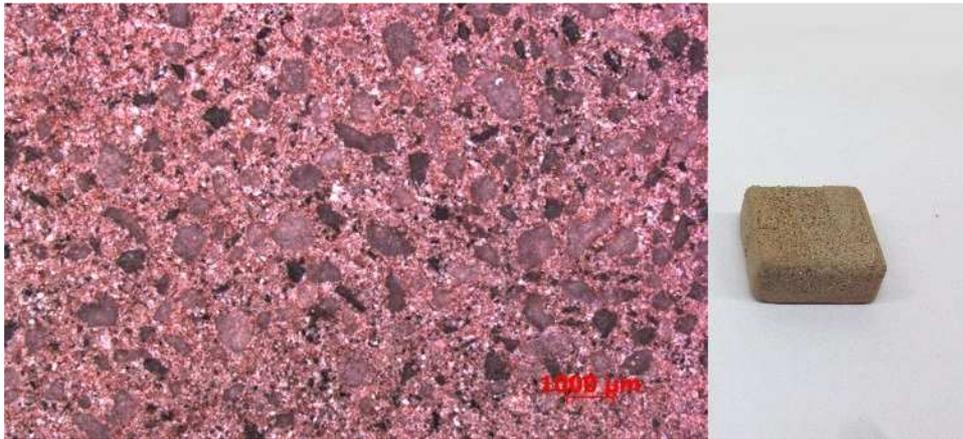
Figure 32. Specimen No.3 after test at 600 °C, commercial ceramics Rescor 750 reinforced with 19 wt.% of basalt powder
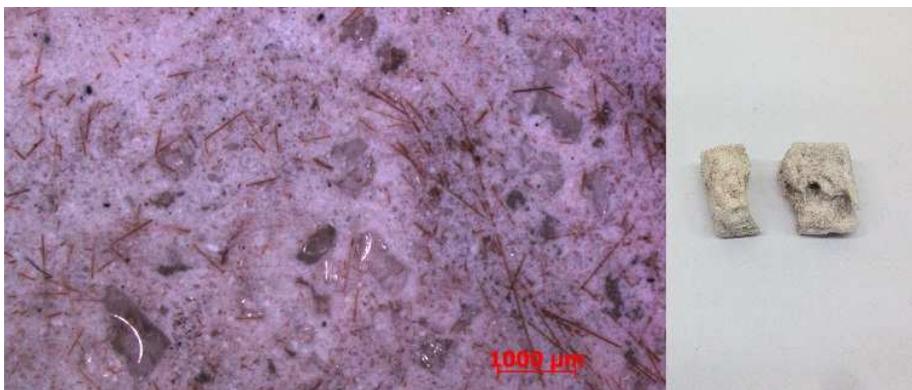
Figure 33. Specimen No.4 after test at 600 °C, commercial ceramics Rescor 750 reinforced with 5 wt.% of basalt fiber
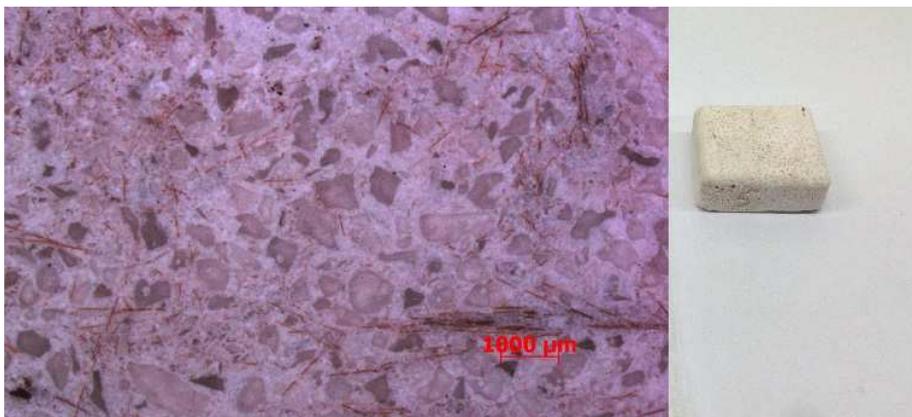
Figure 34. Specimen No.5 after test at 600 °C, commercial ceramics Rescor 750 reinforced with 1 wt.% of basalt fiber

Figure 35. Specimen No.6 after test at 600 °C, commercial ceramics Rescor 750 reinforced with 11wt.% of basalt fiber. Bundles of basalt fiber are visible
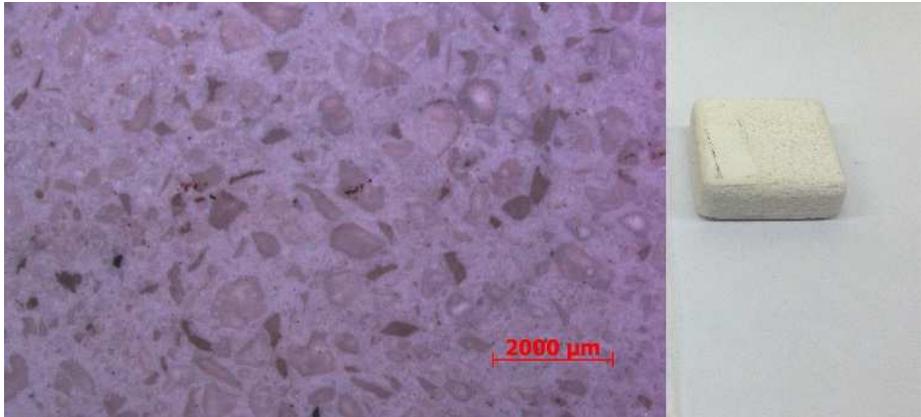
Figure 36. Specimen No.7 after test at 600 °C, commercial ceramics Rescor 750 reinforced with 11 wt.% of Microsil M4
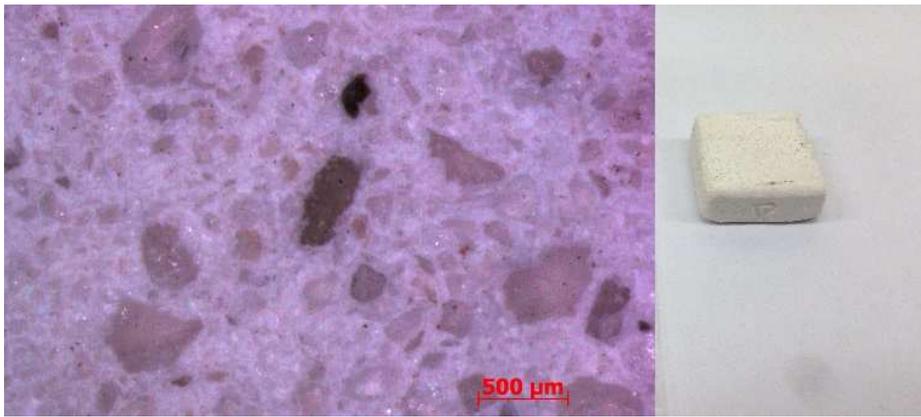
Figure 37. Specimen No.8 after test at 600 °C, commercial ceramics Rescor 750 reinforced with 28 wt.% of Microsil M4
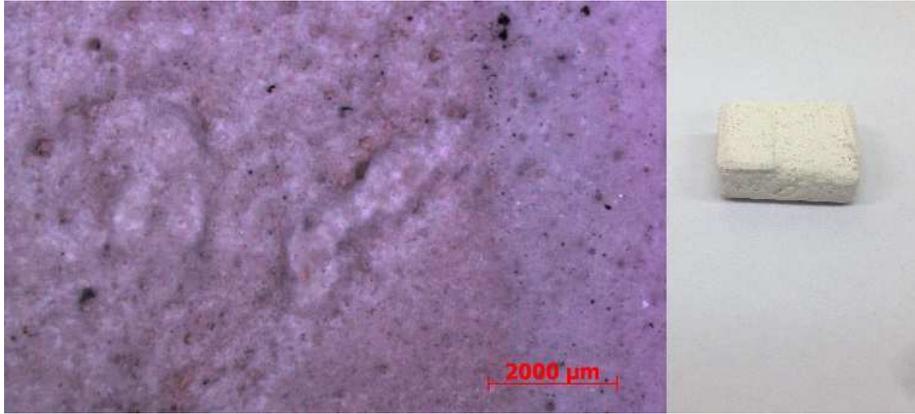
Figure 38. Specimen No.9 after test at 600 °C, commercial ceramics Rescor 750 reinforced with 38 wt.% of Microsil M4
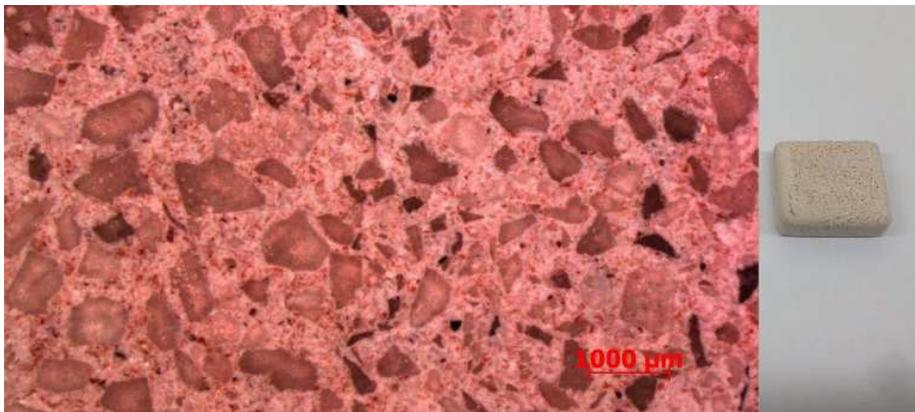
Figure 39. Specimen No.10 after test at 600 °C, commercial ceramics Rescor 750 reinforced with 2 wt.%   of basalt flakes
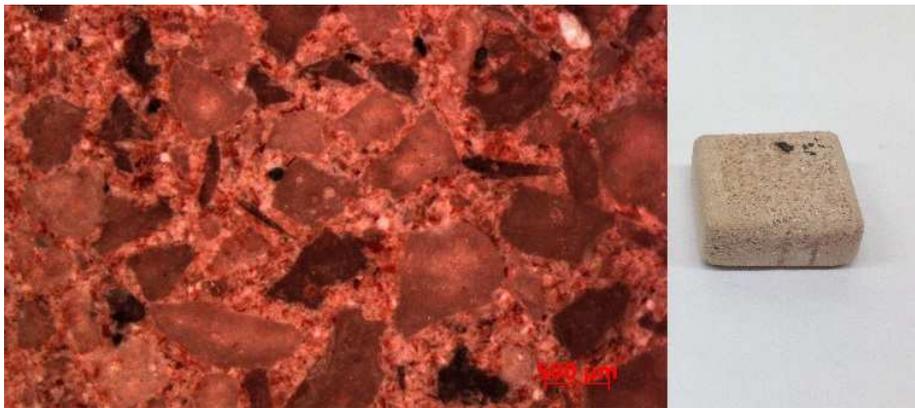
Figure 40. Specimen No.11 after test at 600 °C, commercial ceramics Rescor 750 reinforced with 6 wt.% of basalt flakes
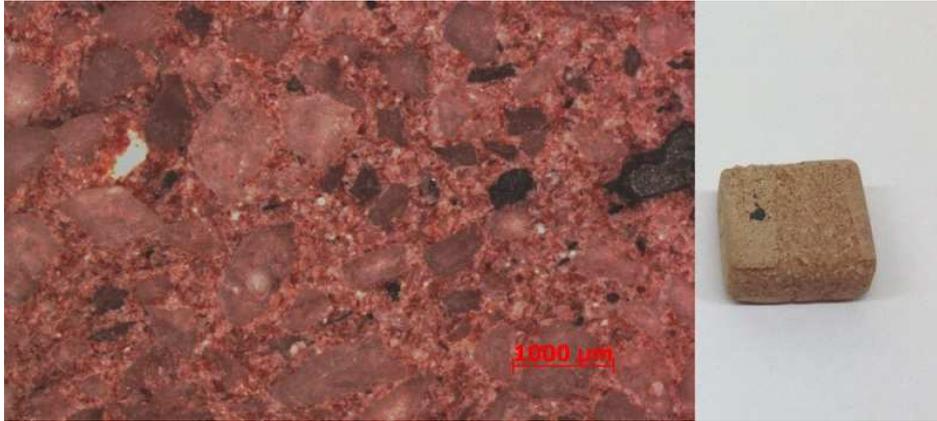
Figure 41. Specimen No.12 after test at 600 °C, commercial ceramics Rescor 750 reinforced with 12 wt.% of basalt flakes

Figure 42. Specimen No.13 after test at 600 °C, commercial ceramics Rescor 780 (based on alumina oxide)

Figure 43. Specimen No.14 after test at 600 °C, commercial ceramics Rescor 780 (based on zirconium oxide)
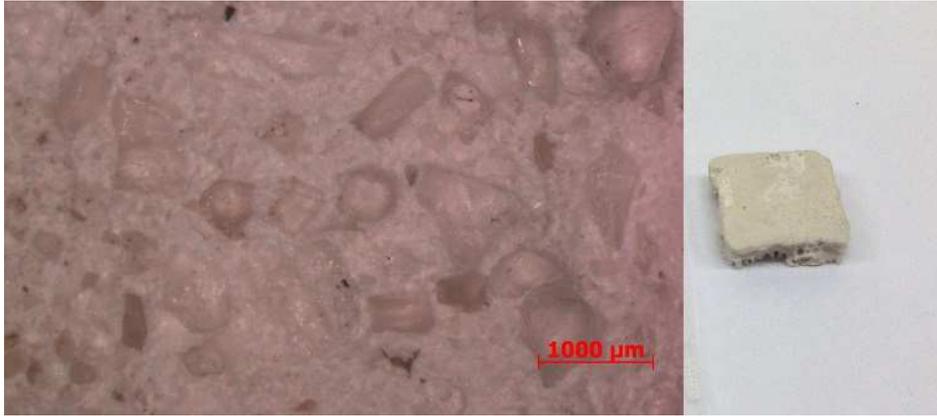
Figure 44. Specimen No.15 after test at 600 °C, liquid glass reinforced with 65 wt.% of basalt powder
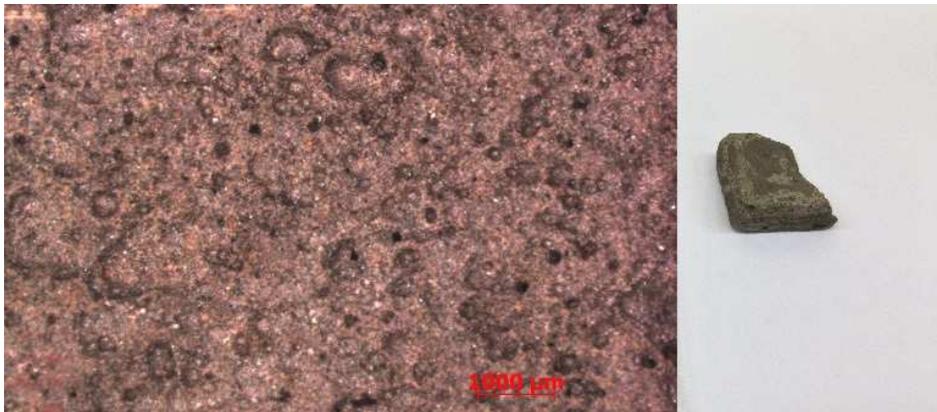
Figure 45. Specimen No.16 after test at 600 °C, liquid glass reinforced with 65 wt.% of basalt flakes
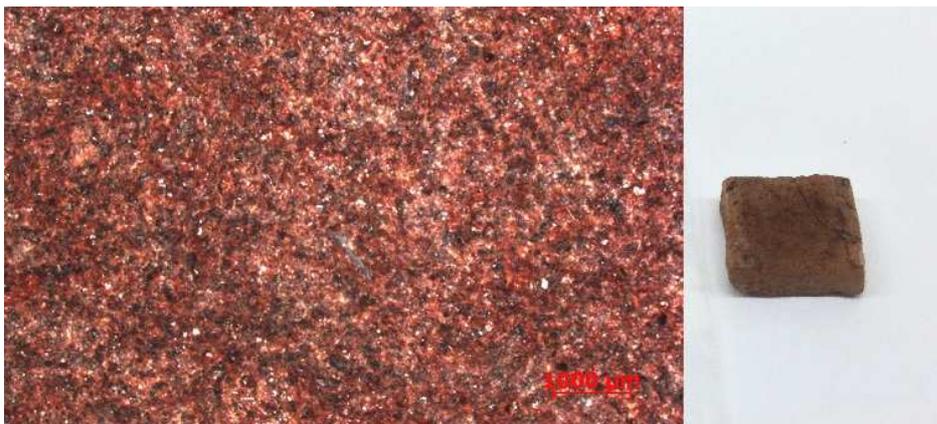
Figure 46. Specimen No.17 after test at 600 °C, liquid glass reinforced with 65 wt.% of sand Microsil M4
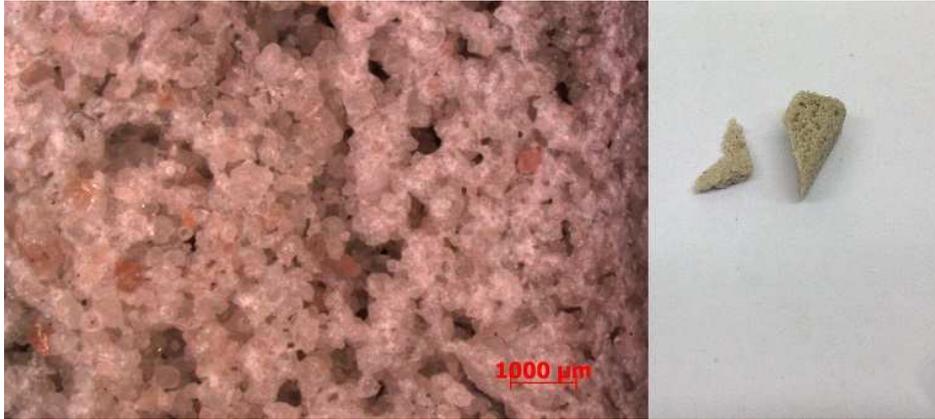
Figure 47. Specimen No.18 after test at 600 °C, liquid glass reinforced with 65 wt.% of sand
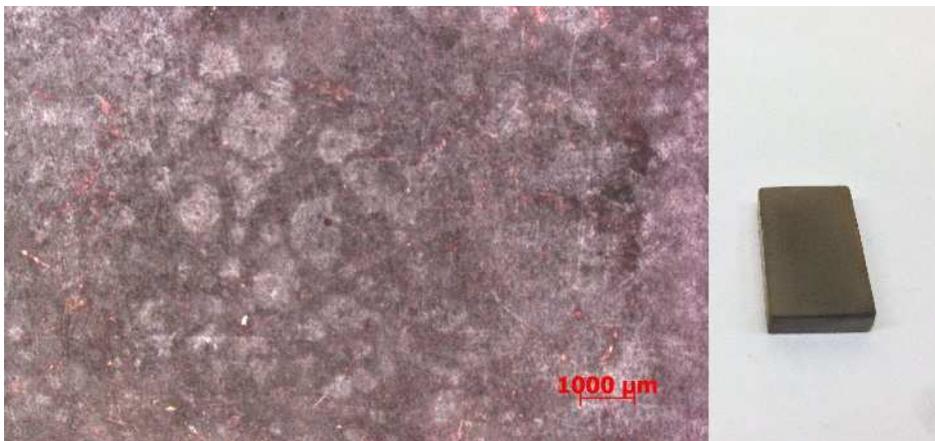
Figure 48. Specimen No.19 after test at 600 °C, steel AISI 316

3.6. Calculation of wear resistance

For testing of samples, centrifugal accelerator for hot erosion testing (model CAK-HET) has been used.
Calculation for loss of weight of tested samples:

$$\Delta M = (m_1 - m_2) \cdot 1000 , \tag{1}$$

where ΔM – loss of weight after erosion test, mg;
m_1 – weight of sample before erosion test, g;
m_2 – weight of sample after erosion test, g.

Calculation for volume of wear of tested samples:

$$V = \Delta M / \rho , \tag{2}$$

where V – volumetric wear, mm^3;
ΔM – loss of weight during erosion test, mg;
ρ – material density, g/mm^3.

3.7. Test results

Twenty specimens had been tested to measure their resistance to solid particle erosion in three different temperature regimes. For more convenient understanding, all specimens are divided into groups according to their microstructure. The first group is commercial castable ceramics from Cotronics: Rescor 750 (SiO_2 base), Rescor 760 (Al_2O_3 base), Rescor 780 (ZrO_2). The highest erosion resistance during three tests was reached by Rescor 780. At 20 °C the wear rate was 26.88 mm^3 (see Figure 49), but in next two tests we can see better resistance. 11.15 mm^3 of wear rate at 300 °C and 10.0 mm^3 at 300 °C was reached by Rescor 780. Another commercial ceramic Rescor 750 has almost the same result at 600 °C – 10.51 mm^3 of wear rate, however, 30.74 mm^3 at 300 °C and 32.90 mm^3 at 300 °C are higher than for the previous one. Specimen with the worst wear resistance was Rescor 760 in all temperature regimes with rates being more than hundred times bigger. Its wear rate was 460.95 mm^3 already after first testing, 359.88 mm^3 at 300 °C and 226.80 mm^3 at 600 °C . Moreover it was cracked and broke into two parts at 600 °C.
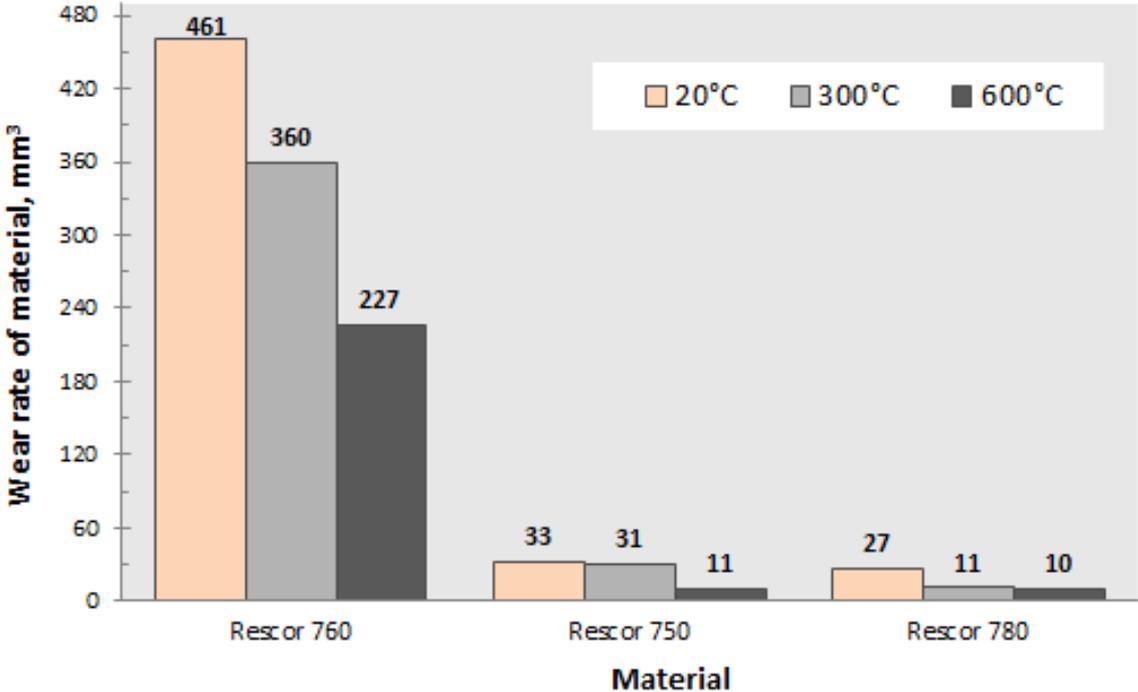
Figure 49. Comparison of wear rates of commercial castable ceramics at different temperatures

The second group of specimens for comparison was group of ceramics made of Rescor 750 and basalt powder. Mixing Rescor 750 with different concentrations of basalt powder gave use positive influence on erosion resistance at all temperature regimes (see Figure 50).

With 7 wt. % of basalt powder at 20 °C wear rate was 31,31 mm^3 which is better by 4,8 % than without reinforcement. After that wear rate began to decrease rapidly, 23,99 mm^3 at 300 °C which is better than commercial by 22 %. During the last testing of the same specimen wear rate did not reached any extraordinary results and was 10,49 mm^3. Addition of 19 wt. % basalt powder helps to reach significant changes already at 20 °C, 30 % (22,99 mm^3) better resistance to erosion. At 300 °C wear rate was 18,01 mm^3 which is better by 41,4 % than Rescor 750. At 600 °C wear rate lowers on approximately 28,8 % (7,51 mm^3) in comparison with two other specimens.
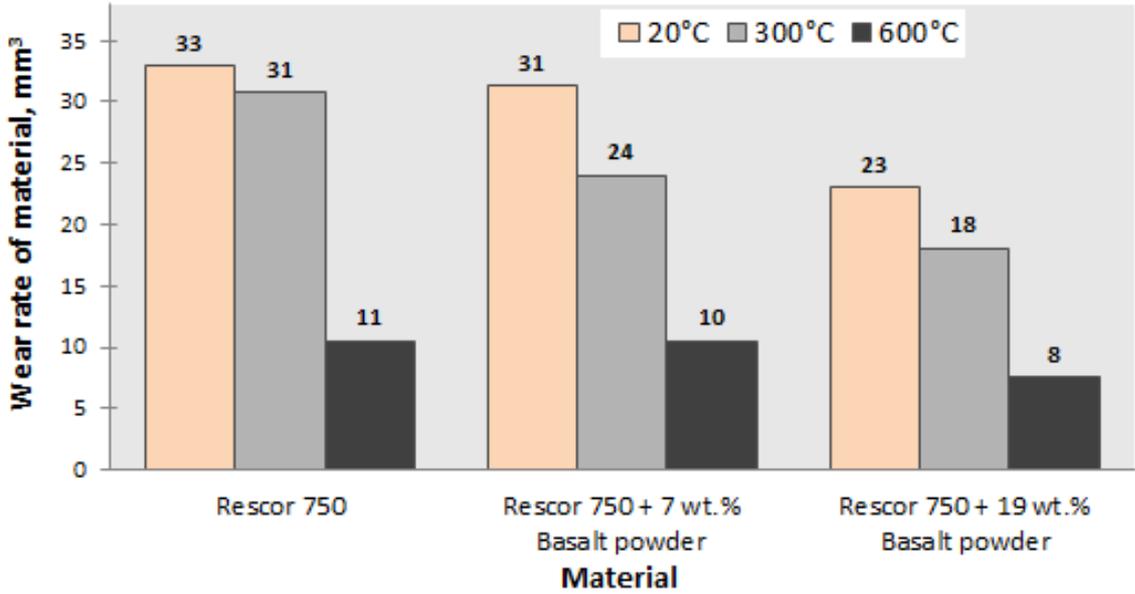
Figure 50. Effect composition of ceramics on wear rate at different temperatures

The next group to be compared with Rescor 750 will be specimens with basalt fibers addition. We can see a tendency towards wear rate increase with increasing concentration of basalt fibers (see Figure 51). Rescor 750 with 5 wt. % of basalt fibers shows at 20 °C increased wear rate in 76,7 % (58,12 mm^3), at 300 °C was already 1284 mm^3. Finally, during 600 °C test this specimen had been failed, worn out in the middle, broken into two parts and wear rate was 133,66 mm^3. Addition of 11 wt.% of basalt fibers shows more negative influence on erosion resistance with wear rate 366,26 mm^3 at 20 °C, 255,26 mm^3 at 300 °C and 17,11 mm^3 at 600 °C. Only lowest content of basalt fibers (1 wt. %) gave improvement in wear resistance at all temperature regimes. Wear rate had reached only 23,95 mm^3 at room temperature, which is better on 27,2 % than commercial sample. At 300 °C wear rate decreased by 44,7 % (17,01 mm^3) and by 32,6 % (7,12 mm^3) during test at 600 °C.
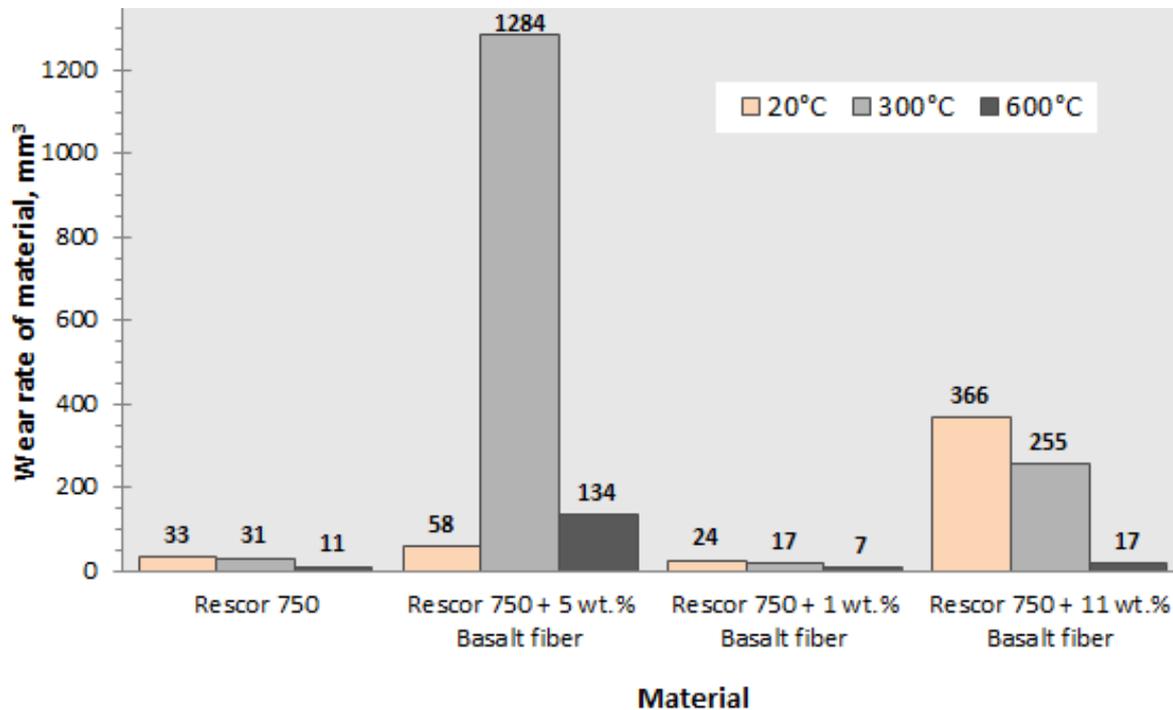
Figure 51. Effect of composition of ceramics on wear rate at different temperatures

According to testing results it is obvious that silica flour Microsil M4 cannot be used as reinforcement, because in general it has negative influence on erosion resistance at all temperature regimes. We can see tendency towards wear rate increasing with increasing concentration of M4 (see Figure 52). Room temperature test with 11 wt. % M4 shows 21,6 % (40,0 mm^3) worse wear resistance than Rescor 750 has (32,9 mm^3), and 28,1 % (13,49 mm^3) worse at 600 °C comparison with Rescor 750 (10,51 mm^3), except testing at 300 °C – 16,61 mm^3 that is better on 46 %. Specimen with 28 wt. % M4 has wear rate 72,08 mm^3 at 20 °C, 38,38 mm^3 at 300 °C, 11,25 mm^3 at 600 °C. Lowest resistance against erosion had ceramics with 38 wt. % of Microsil M4: 104,33 mm^3 at 20 °C, 118,93 mm^3 at 300 °C, 56,13 mm^3 at 600 °C.
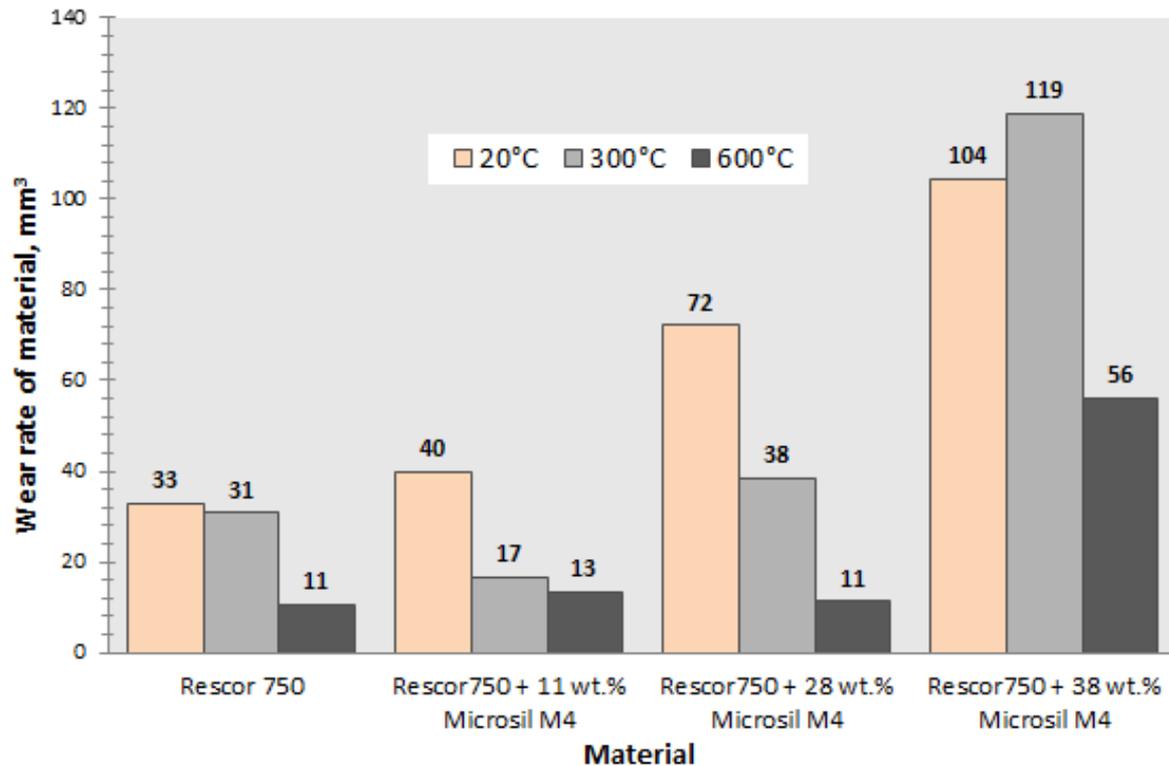
Figure 52. Effect of composition of ceramics on wear rate at different temperatures

We can see similar wear resistance of ceramics with basalt flakes and with basalt fibers. Samples with highest concentration of fibers, approximately 12 wt. % had higher wear rate by 71,5 % (56,44 mm^3) at 20 °C, 84,3 % (56,65 mm^3) at 300 °C, 134,8 % (24,71 mm^3) at 600 °C (see Figure 53). With lower level fibers (6 wt.%) wear rate becomes lower, but nevertheless higher on 25,8 % (41,37 mm^3) at 20 °C, on 29,9 % (13,68 mm^3) at 600 °C than pure Rescor 750, except lower wear rate on 6,7 % (28,68 mm^3) at 300 °C. Increased erosion resistance by 3,1 % (31,86 mm^3) at 20 °C, 53,9 % (14,18 mm^3) at 300 °C, 34,7 % (6,89 mm^3) at 600 °C was shown by specimen with 2 wt. % .
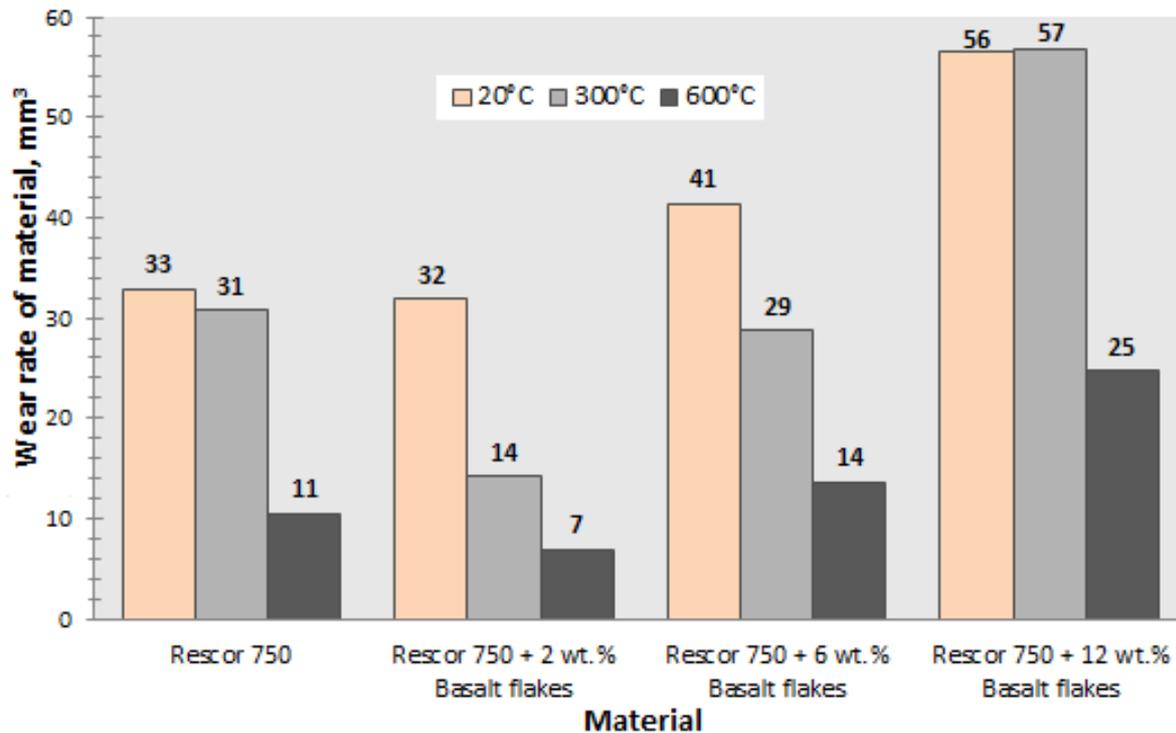
Figure 53. Effect of composition of ceramics on wear rate at different temperatures

The next group of tested specimens to be compared with commercial ceramics in erosion resistance is based on liquid glass with additions of basalt and sand. It should be noted that all samples in this group had cracked during removal after wear test at 600 °C, except liquid glass with sand, which had cracked even earlier (after test at 300 °C). For sample with sand it was impossible to measure its loss of weight properly (see Figure 54). Low wear resistance can be explained by very porous and brittle structure of liquid glass. In spite of this fact specimen with addition of 65 wt. % basalt flakes had shown much better wear resistance up to 37,1 % (20,68 mm^3) at 20 °C, 27,2 % (7,68 mm^3) at 600 °C than commercial ceramics Rescor 750, except 45,96 mm^3 of wear rate at 300 °C, which is on 49,5 % worse. Liquid glass with basalt powder had shown 8,84 mm^3 of wear rate at 20 °C, which is on 73,1 % better than Rescor 750. However, at 300 °C wear rate was 55.72 mm^3, at 600 °C wear rate was 318,96 mm^3 which are significantly bigger. The highest wear rate was 437,36 mm^3 at 300 °C in case of Microsil M4 addition. The same specimen at 20 °C had wear rate 49,24 mm^3 which is on 49,7 % worse than Rescor 750, and 31,88 mm^3 wear rate at 600 °C, which is on 203 % worse than Rescor 750.
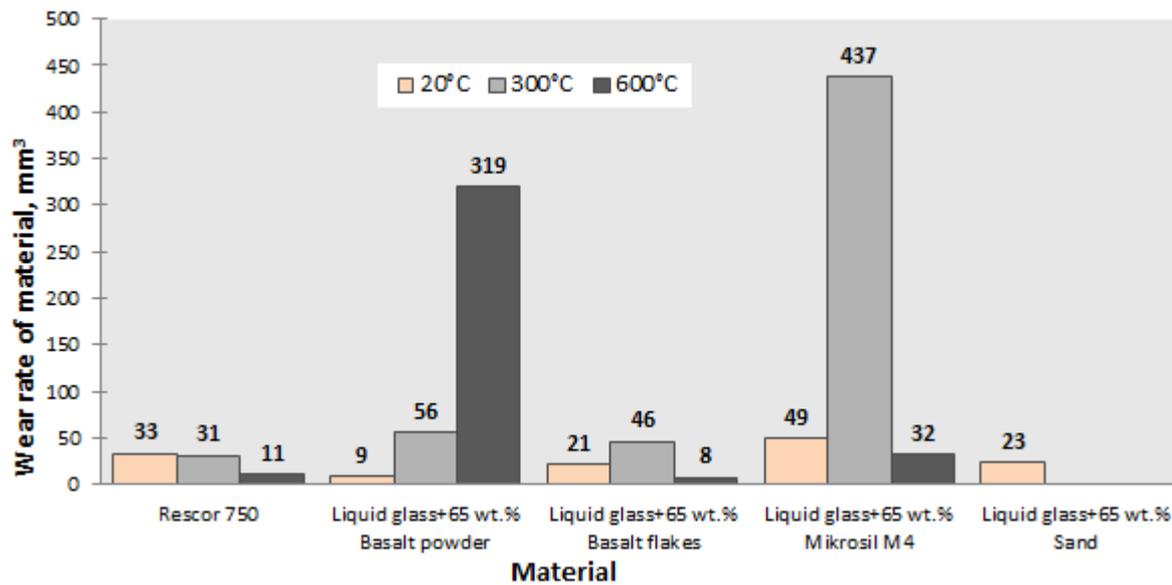
Figure 54. Effect of composition of ceramics on wear rate at different temperatures

In Figure 55, the wear rates of specimens with best erosion resistance from each group of additives are shown. We can see that there is no absolutely perfect sample suitable for all temperature regimes. However, it should be noted that all three specimens based on Rescor 750 and liquid glass with reinforcement additives have better wear resistance by 25 % (R750 + basalt powder 7,51 mm^3; R750 + basalt fiber 7,12 mm^3; R750 + basalt flakes 6,89 mm^3; Liquid glass + basalt flakes 7,68 mm^3) at 600 °C than commercial ceramics with lowest wear rates. Same specimens, except R750 with basalt flakes, have better erosion resistance at 20 °C test. Only at 300 °C commercial Rescor 780 with 11,15 mm^3 wear rate has better wear resistance than all other samples.
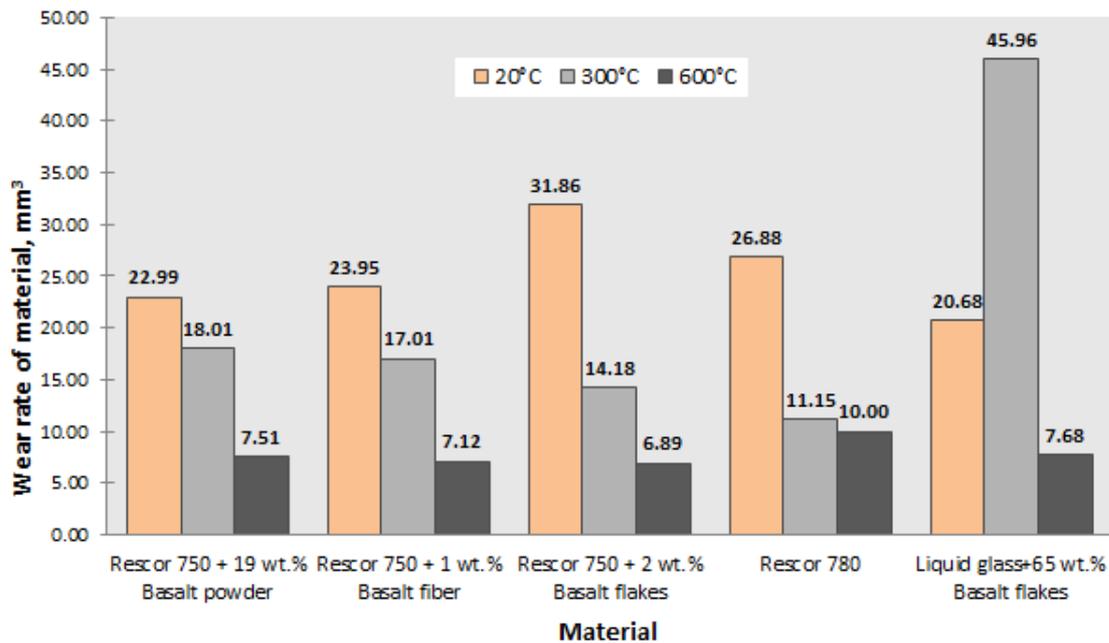
Figure 55. Comparison between the best reinforced specimens with commercial one

CONCLUSIONS

All testing processes from designing and producing of specimens to last test at 600 °C, was performed as planned. Used equipment provided comfortable and stable work. The experimental part of this work lasted about one month and all aims were reached.

For better understanding, results of erosion tests of stainless steel AISI 316 were also included into testing. As was supposed, cast ceramic materials do not have sufficient resistance in solid particle erosion resistance due to their brittleness if compare with ductile material like stainless steel. The worst wear rate value of steel was approximately 47 times lower than the best wear rate value of ceramics (see Figure 56). Our efforts were aimed at erosion resistance research and improvement of commercially available castable ceramics from Cotronics corporation: Rescor 750 based on SiO_2; Rescor 780 based on Al_2O_3; Rescor 760 based on ZrO_2. In fact, only Rescor 750 and Rescor 780 are suitable for solid particle erosion up to 600 °C, because Rescor 760 had very high wear rates. However, was reached results in decrease of wear rate of commercial ceramics by adding reinforcement agent (various concentrations and types of basalt materials: basalt powder, basalt fibers, basalt flakes).
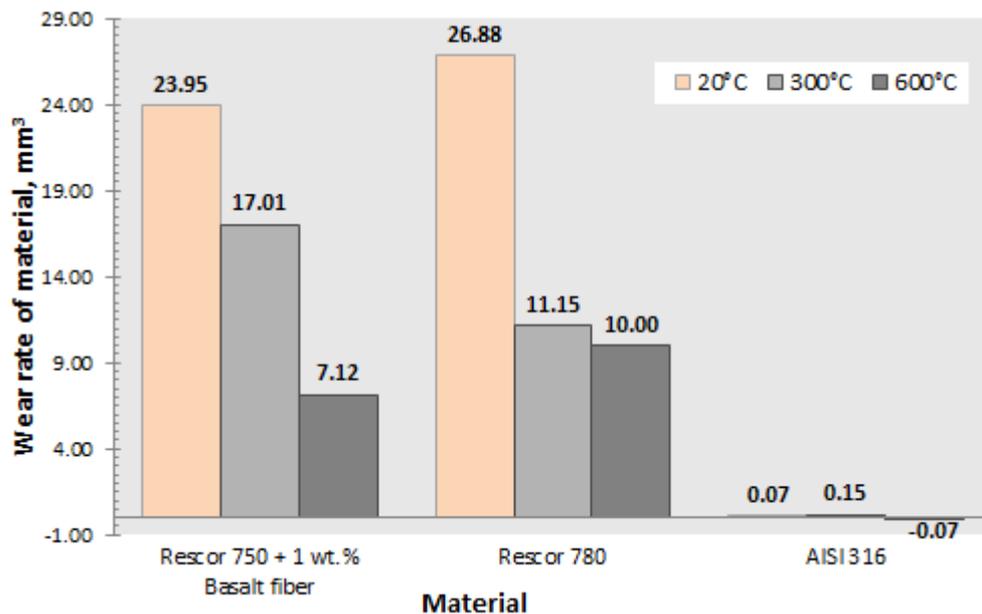
Figure 56. Comparison of wear rates between castable ceramics (Rescor 750 reinforced with basalt fibers, commercial Rescor 780) and stainless steel (AISI 316)

Addition of 1 wt. % of basalt fiber, in commercial ceramics Rescor 750, allowed to raise wear resistance up to 27,2 % at 20 °C testing, 44,7 % at 300 °C testing, and 32,6 % at 600 °C testing.

Addition of 19 wt. % of basalt powder, in commercial ceramics Rescor 750, raised wear resistance up to 30 % at 20 °C testing, 41,4 % at 300 °C testing, and 28,8 % at 600 °C testing.

Addition of 2 wt. % of basalt flakes, in commercial ceramics Rescor 750, raised wear resistance up to 3,1 % at 20 °C testing, 53,9 % at 300 °C testing, and 34,7 % at 600 °C testing.

It is necessary to make further research in the field of castable ceramic reinforcement, because it can be perspective direction to creation of cheap and available ceramic materials which can be useful at high temperature applications in presence of solid particle erosion. Obtained from commercial, a new type of castable ceramics based on SiO_2 and reinforced by basalt materials can be used as a material for supporting construction for heating springs in the new erosion tester that will be build in Tallinn University of Technology.

Simultaneously there was designed new type of ceramics based on liquid glass and reinforced by: basalt fibers, basalt flakes and sand. This type of ceramics is cheaper and available for use than commercial castable ceramics from Cotronics corp. Although some specimens with liquid glass ceramics had been broken after test at 600 °C, other samples showed high wear resistance.

Addition of 65 wt. % of basalt powder made by using disintegrator, with liquid glass, during testing at 20 °C allowed to reach wear resistance higher by 73,1 % (8,82 mm^3) than commercial ceramics Rescor 750.

Addition of 65 wt. % of basalt flakes from company Otselot, in liquid glass, during testing at 20 °C allowed to reach wear resistance higher by 37,1 %, at 600 °C higher by 27,2 % than commercial ceramics Rescor 750.

Specimens with liquid glass reinforced by sand or crystalline flour by Sibelco cannot be perspective in this type of applications. They had shown high erosion rate and broken down during the disinstallation. Liquid glass with sand was broken down after the test at 20 °C and liquid glass with crystalline flour was broken down after the test at 600 °C.

Liquid glass ceramics with basalt produced in Tallinn University of Technology can compete with commercial ceramics from Cotronics in solid particle erosion conditions. It is necessary to make research of new compositions of reinforced liquid glass ceramics in order

to find more stable and cheaper materials that can be used in high temperature applications in the presence of erosion.

Introduction of new installation way of specimens on specimen ring with special wedge was successful and allowed a stable testing. It can be accepted as reliable and more convenient method that can be used in further erosion tests of weak samples.

According to the results of tests, ceramic Rescor 750 reinforced with 1 wt. % of basalt fiber and ceramic Rescor 750 reinforced of 19 wt. % of basalt powder are suitable materials for supporting elements of heating springs and could be used in new erosion tester.

KOKKUVÕTE

Kõik etapid, alustades katsekehade valmistamist kuni viimase katsetuseni, olid viidud läbi plaani järgselt.

Praktiline osa koosnes katsekehade valmistamisest ja nende katsetamisest. Katsekehade paagutamiseks kasutati laboratoorset ahju Nabertherm L9/13 P330 kontrolleriga, mis on võimeline saavutama ja hoidma temperatuuri kuni 1300 °C. Katsetuste läbiviimiseks kasutati TTÜ-s valmistatud seadet CAK- HET (töötab sarnaselt GOST 23.201-78.1978 standardis mainitud masinaga, aga võimaldab katsetada ka kõrgtemperatuuridel). Katsetused viidi läbi kolmes etapis katsetamisega temperatuuridel 20 °C, 300 °C, 600 °C erosiooni keskkonnas. Kasutatud seadmed võimaldasid mugavat ja stabiilset tööd. Praktiline osa jätkus umbes kuu aega ja kõik eesmärgid saavutati.

Võrdluseks katsetati ka roostevaba terast (AISI 316). Terase erosioonikindlus oli tunduvalt suurem, kui valamistehnoloogia abil saadud keraamiliste materjalide oma. Valamistehnoloogia abil saadud keraamika mehaanilised omadused on madalamad kui täispaagutatud tavalise keraamika omad. Kuna valatud keraamika põhiline kasutusvaldkond on elektrilised isolaatorid ja kuumuskindlad tugielemendid, siis nende kasutusvaldkondade jaoks on nende tugevusomadused piisavad. Kahjuks on keraamilised materjalid väga tundlikud defektide vastu ja defektide olemasolul nende tugevusomadused langevad märgatavalt. Valamistehnoloogia abil saadud keraamika ei sula valmistamisprotsessi jooksul ja seetõttu jääb materjali struktuuri hulgaliselt poore, mis soodustab materjali haprust ning purunemist kokkupõrkel erosiooni osakestega. Roostevaba terase kõige suurem kulumise väärtus oli umbes 47 korda väiksem kui valatud keraamika kõige madalam kulumise väärtus (vt Sele 56).

Käesoleva töö eesmärgiks oli laialdaselt kasutatava valmistustehnoloogia abil saadud keraamika erosioonikindluse tõstmine. Uuringutel kasutati tööstusliku keraamikat firmalt *Cotronics*: Rescor 750 (põhikomponent SiO_2); Rescor 780 (põhikomponent Al_2O_3); Rescor 760 (põhikomponent ZrO_2). Eelpool nimetatud materjalidest katsetati vaid Rescor 750 ja Rescor 780 temperatuuril 600 °C, sest Rescor 760 kulus väga intensiivselt. Häid tulemusi tööstusliku keraamika kulumise vähendamises saavutati tänu katsekeha struktuuri tugevdamisele basalti lisanditega. Valmistati ja katsetati erinevad basalti tugevdavate lisandite kujusid (helbeid, osakesi, kiude) ja nende kontsentratsioone, mis on unikaalne. Selle töö tulemusena kirjutati artikkel „Erosive wear resistance of castable ceramics" BaltMatTrib2015 konverentsi jaoks.

Leiti, et 1 mass % basaltkiudude lisamine keraamikasse Rescor 750, võimaldab suurendada kulumiskindlust 27 %, 45 % ja 33 % katsetamisel temperatuuril 20 °C, 300 °C ja 600 °C.

Leiti, et 2 mass % basalthelbede lisamine keraamikasse Rescor 750, võimaldab suurendada kulumiskindlust 3 %, 54 % ja 35 % katsetamisel temperatuuril 20 °C, 300 °C ja 600 °C.

Leiti, et 19 mass % basaltpulbri lisamine keraamikasse Rescor 750, võimaldab suurendada kulumiskindlust 30 %, 41 % ja 29 % katsetamisel temperatuuril 20 °C, 300 °C ja 600 °C.
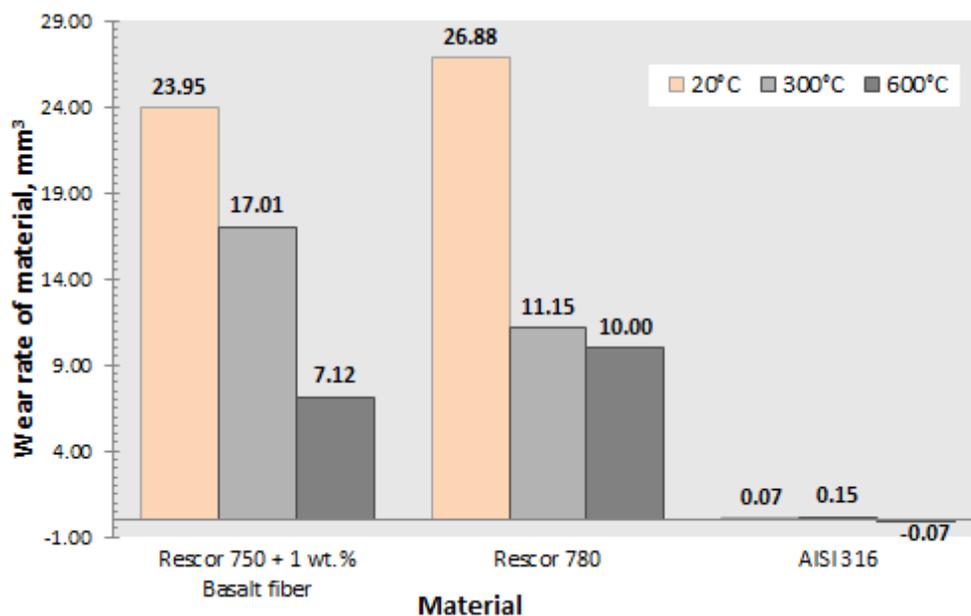
Sele 56 (koopia). Keraamika katsekehade (Rescor 750 tugevdatud basalti kiududega, Rescor 780) ja roostevaba terase AISI 316 kulumise võrdlus

On soovitatav jätkata alustatud uuringuid, tööstusliku valamistehnolooga abil saadud keraamiliste materjalide omaduste optimeerimiseks, erosioonkindluse suurendamiseks tänu basalti lisanditele. Sellest võib tulla edasiulatuv suund kättesaadavate ja odavate keraamika materjalide valmistamiseks, mis leiavad aset erosiooni tingimustes kõrgetel temperatuuridel.

Teiseks põhisuunaks oli komposiitmaterjalide loomine vedeliku klaasi baasil basaldi (helbed või kiud) ja liiva lisanditega. See keraamika on palju odavam ja kättesaadavam, kui *Cotronics*-i oma. Mõned materjalid olid väga tõsiselt kulunud aga mõned näitasid head kulumiskindlust võrreldes *Cotronics*-i baasil valmistatud materjalidega.

Leiti, et 65 mass % basaldi pulbri lisamine vedeliku klaasi võimaldab saavutada 73 % kõrgemat kulumiskindlust võrreldes Rescor 750 materjaliga juhul kui katse viiakse läbi temperatuuril 20 °C.

Leiti, et 65 mass % basaldi helbete lisamine vedeliku klaasi võimaldab saavutada 37 % ja 27 % kõrgemat kulumiskindlust võrreldes Rescor 750 materjaliga juhul kui katse viiakse läbi temperatuuril 20 °C või 600 °C.

Komposiitmaterjalide valmistamine vedeliku klaasi ja jäme- või peen(*Sibelco*) liivaga ei ole sobilik kasutamiseks erosioonkeskkonnas kõrgetel temperatuuridel. Nende materjalide kulumine oli suur ning materjalide madala tugevuse tõttu purunesid nad tihti kinnitamise või välja võtmise käigus. Katsekeha jämeliivaga purunes temperatuuril 20°C ja katsekeha peenliivaga purunes peale katsetamist temperatuuril 600 °C.

Keraamika vedeliku klaasi alusel basaldi lisanditega, mis loodi Tallinna Tehnikaülikoolis, võiks luua konkurentsi tööstusliku keraamikale firmale *Cotronics*, kui kasutada neid erosiooni keskkonnas. Tulenevalt sellest on vaja jätkata uuringuid teatud valdkonnas ja otsida uusi vedeliku klaasi basalti tugevdavate lisandite kombinatsioone erosioonikindluse tõstmiseks.

Habraste katsekehade paigaldamiseks erosioonmasinasse töötati välja uus kinnitusmeetod. Katsete läbiviimiseks temperatuuril 20°C kasutati pehmest puidust kiile, mis paigaldati hoidiku ja klambrite vahel. Katsetamiseks kõrgetel temperatuuridel puukiilud ei sobinud ja sellepärast sai loodud õhukesest (0.5 mm) metalllehest valmistatud vedrukiil. Vedrukiilu valmistamiseks metallist leht painutati keskelt väikse nurga all. Teravad ääred olid eemaldatud. Niisugune vedrukiil võimaldab hoolikat kinnitada haprad keraamilised katsekehad ja välistada nende purunemist termiliste pingete tõttu. Pakutud vedrukiil fikseeris katsekeha stabiilselt ning seda oli lihtne kasutada. Soovitakse seda kasutada ka tuleviku katsetamises.

Arvestades esitatud tulemusi võib järeldada, et keraamilised materjalid, mis on valmistatud valamismeetodiga basaldi tugevdusfaasi lisamisega (Rescor 750 koos 1 mass % basaldi kiududega ja Rescor 750 tugevdatud 19 mass % basaldi pulbriga) sobivad kasutamiseks (tugielementidena küttespiraalide asetamiseks) uues erosiooni kastemasinas, mida luuakse praegu Tallinna Tehnikaülikoolis.

REFERENCES

1. ASM Handbook. Friction, Lubrication, and Wear Technology. Volume 18. USA: 1992.

2. D. J. Buquoi. Solid Particle Erosion: Its Causes, Effects and Solutions. USA: 1989.

3. T.H. McCloskey, C. Bellanca. Minimizing Solid Particle Erosion in Power Plant Steam Turbines. – Power Engineering, 1981, 35-38

4. A. Garton, W.T.K. Stevenson, P.D. McLean. The Stability of Polymers in Low Earth Orbit. - Materials and Design, 1986, 7, 319-323

5. W. A. Glaesser. Materials for tribology. USA: Elsevier, 1992.

6. G. Sundararajan, P.G. Shewmon. A new model for the erosion of metal at normal incidence. – Wear, 1983, 84, 237-258

7. I.V. Kragelsky, A.I. Zolotar, A.O. Sheiwekham. Theory of material wear by solid particle impact. – Tribology, 1985, 18, 3-11

8. G.W. Stachowiak, A.W. Batchelor. Engineering tribology. Third edition. USA: Elsevier, 1992.

9. A.W. Ruff, S.M. Wiederhorn. Erosion by Solid Particle Impact. USA: Defence Technical Information Center, 1979.

10. I.M Hutchings. Tribology: Friction and wear of engineering materials. Cambridge: Butterworth-Heinemann Ltd, 1992.

11. M.A. Moore, F.S. King. Abrasive Wear of Brittle Solids. - Wear, 1980, 60, 123-140

12. B.R. Lawn, M.V. Swain. – Journal of material science, 1975, 10, 113-122

13. K.Zum Gahr. Microstructure and wear of materials. New York, 1987.

14. I.M Hutchings. Chemical engineering science, 1987, 42, 869-878

15. J.H. Neilson, A. Gilchrist. Erosion by a stream of solid particles. – Wear, 1968, 11, 111-123

16. J.E. Goodwin, W. Sage, G.P. Tilly. Study of Erosion by Solid Particles. - Proceedings of the Institution of Mechanical Engineers, 1969, 184, 279-289

17. S. Bahadur, R. Badruddin. Erodent Particle Characterization and the Effect of Particle Size and Shape on Erosion. - Wear, 1990, 138, 189-208

18. T.H. Kosel, A.P.L. Turner, R.O. Scattergood. Effects of Particle Size and Shape on Erosive Wear Mechanisms. - Corrosion-Erosion Behaviour of Materials, 1980, 146-161

19. I.M. Hutchings, W.F. Adler. Erosion: Prevention and Useful Applications. 3-rd ed., USA: 1979.

20. M.G. Hamblin, G.W. Stachowiak. A Multi-Scale Measure of Particle Abrasivity. - Wear, 1995, 185, 225–233

21. G.W. Stachowiak, M.G. Hamblin. A Multi-Scale Measure of Particle Abrasivity and Its Relation to Two Body Abrasive Wear. - Wear, 1995, 190, 190–196

22. G.W. Stachowiak. Wear – Materials, Mechanisms and Practice. England: John Wiley & Sons, 2005.

23. M.G. Hamblin, G.W. Stachowiak. Description of Abrasive Particle Shape and Its Relation to Two-Body Abrasive Wear. - Tribology Transactions, 1996, 39(4), 803–810

24. G.W. Stachowiak. Numerical Characterization of Wear Particle Morphology and Angularity of Particles and Surfaces. London: MEP Publications Ltd., 1997.

25. A. Misra, I. Finnie. On the Size Effect in Abrasive and Erosive Wear. - Wear, 1981, 65, 359-373

26. G.L. Sheldon, I. Finnie. On the Ductile Behaviour of Nominally Brittle Materials During Erosive Cutting. - Transactions ASME, 1966, 88B, 387-392

27. J.G.A. Bitter. A Study of Erosion Phenomena. - Wear, 1963, 6, 5-21

28. R. Brown, E.J. Jun, J.W. Edington. Erosion of α – Fe by spherical glass particles. – Wear, 1981, 70, 347 -363

29. K. Anand, S.K. Hovis, H. Conrad, R.O. Scattergood. Flux Effects in Solid Particles Erosion. - Wear, 1987, 118, 243-257

30. J.C. Arnold, I.M. Hutchings. Flux Rate Effects in the Erosive Wear of Elastomers. - Journal of Materials Science, 1989, 24, 833-839

31. T.H. Kosel, R.O. Scattergood, A.P.L. Turner. An Electron Microscope Study of Erosive Wear. USA: American Society of Mechanical Engineers, 1979.

32. I. Finnie, J. Wolak, Y.H. Kabil. Erosion of metals by solid particles. – Journal of Materials, 1967, 2, 682-702

33. S. Dosanjh, J.A.C. Humphrey. The Influence of Turbulence on Erosion by a Particle-Laden Fluid Jet. - Wear, 1985, 102, 309-330

34. A.V. Levy, G. Hickey. Liquid-Solid Particle Slurry Erosion of Steels. - Wear, 1987, 117, 129-158

35. W. Tabakoff. Study of Single-Stage Axial Flow Compressor Performance Deterioration. - Wear, 1987, 119, 51-61

36. Y. Shida, H. Fujikawa. Particle Erosion Behaviour of Boiler Tube Materials at Elevated Temperature. - Wear, 1985, 103, 281-296

37. D.J. Stephenson, J.R. Nicholls, P. Hancock. Particle-Surface Interactions During the Erosion of a Gas Turbine Material (MarM002) by Pyrolytic Carbon Particles. - Wear, 1986, 111, 15-29

38. A.V.Levy, Y-F. Man. Surface Degradation of Ductile Materials in Elevated Temperature Gas-Particle Streams. - Wear, 1986, 111, 173-186

39. J. Zhou, S. Bahadur, Further Investigations on the Elevated Temperature Erosion-Corrosion of Stainless Steels. - Proceedings of Conference on Corrosion-Erosion-Wear of Materials at Elevated Temperatures, A.V. Levy, Ed., 1990.

40. V.K. Sethi, R.G. Corey. High Temperature Erosion of Alloys in Oxidizing Environments. - Proceedings of 7th International Conference on Erosion by Liquid and Solid Impact, J.E. Field and J.P. Dear, Ed., 1987.

41. H.H. Uhlig. Corrosion and Corrosion Control. Second edition. England: John Wiley & Sons, 1971.

42. C.T. Kang, S.L. Chang, F.S. Petit, N. Birks. Synergism in the Degradation of Metals Exposed to Erosive High Temperature Oxidizing Temperatures. - Proceedings of Conference on Corrosion-Erosion-Wear of Materials at Elevated Temperatures, A.V. Levy, Ed., 1986.

43. C.T. Kang, F.S. Petit, N. Birks. Mechanisms in the Simultaneous Erosion-Oxidation Attack of Nickel and Cobalt at High Temperature. - Metallurgical and Materials Transactions, 1987, 18A, 1785-1803

44. D.M. Rishel, F.S. Petit, N. Birks. Some Principal Mechanisms in the Simultaneous Erosion and Corrosion Attack of Metals at High Temperature. - Proceedings of Conference on Corrosion- Erosion-Wear of Materials at Elevated Temperatures, A.V. Levy, Ed., 1990.

45. Kenneth G. Budinski. Guide to Friction, Wear, and Erosion Testing. USA: ASTM, 2007.

46. B. Basu, K. Balani. Advanced Structural Ceramics. USA: John Wiley & Sons, 2011.

47. G.W. Stachowiak. Wear – Materials, Mechanisms and Practice. England: John Wiley & Sons, 2005.

48. B. Basu, M. Kalin. Tribolgy of ceramics and composites. USA: John Wiley & Sons, 2011.

49. J.F. Lynch, C.G. Ruderer, W.H. Duckworth. Engineering Properties of Selected Ceramic Materials. USA: American Ceramic Society, 1966.

50. I. Finnie. The Mechanisms of Erosive Wear in Ductile Metals. - Corrosion-Erosion Behavior of Materials, 1980, K. Natesan, Ed., 118-126

51. J.S. Hansen. Relative Erosion Resistance of Several Metals. - Erosion: Prevention and Useful Applications, 1979, STP 664, 148-162

52. K.F. Dufrane. Sliding Performance of Ceramics for Advanced Heat Engines. - Ceramic Engineering and Science Proceedings, 1986, (7-8), 1052-1059

53. R. Komanduri, S. Samanta. Ceramics, Metals Handbook. Vol. 16, ninth edition. USA: ASM, 1989.

54. J.C. Arnold, I.M. Hutchings. The Mechanisms of Erosion of Unfilled Elastomers by Solid Particle Impact. - Wear, 1990, 138, 33-46.

55. A.V. Levy. The Solid Particle Erosion Behaviour of Steel as a Function of Microstructure. - Wear, 1981, 68, 269-287

56. G. Lewis, PH-55A: Corrosion, Erosion and Abrasion. - Source Book on Stainless Steels, 1976, ASM Engineering Bookshelf, 62-63

57. P.V. Rao, D.H. Buckley. Angular Particle Impingement Studies of Thermoplastic Materials at Normal Incidence. - ASLE Transactions, 1986, 29, 283-298

58. K.V. Pool, C.K.H. Dharan, I. Finnie. Erosive Wear of Composite Materials. - Wear, 1986, 107, 1- 12

59. R.Crawford. Plastics and Rubber, Engineering Design and Applications. London: Mechanical Engineering Publications, 1985.

60. O.H. Wyatt, D.D. Hughes. Metals, Ceramics and Polymers. London: Cambridge University Press, 1974.

61. S.F. Wayne, J.G. Baldoni, S.T. Buljan. Abrasion and Erosion of WC-Co With Controlled Microstructures. - Tribology Transactions, 1990, 33, 611-617

62. S. Srinivasan, R.O. Scattergood. Erosion of Transformation Toughening Zirconia by Solid Particle Impact. – Advanced Ceramic Materials, 1988, 3, 345-352

63. A.V. Levy, P. Clark. The Erosion Properties of Alloys for the Chemical Industry. - Wear, 1991, 151, 337-350

64. B. Bhushan. Modern Tribology Handbook. Two Volume Set. USA: CRC Press, 2000.

65. T. A. Parthasarathy, R. J. Kerans, S. Chellapilla, A. Roy. Analysis of ceramics toughened by non-conventional fiber reinforcement. - Materials Science and Engineering: A, 2007, 443, 120–131

66. V. Fiore, T. Scalici, G. Di Bella, A. Valenza. A review on basalt fibre and its composites. - Composites Part B: Engineering, 2015, 74, 74–94

67. Использование жидкого стекла в производстве строительных материалов, БГТУ, 2008.

68. В.А. Лотов, В.А. Кутугин, В.В. Ревенко. Термопеносиликатные изделия на основе жидкого стекла и базальтовой чешуи. Томский Политехнический Университет, 2008.

69. AS Kemiakaubandus kodulehekülg [WWW] http://keemiakaubandus.ee/en (17.03.2015).

70. Alfa Aesar kodulehekülg [WWW] https://www.alfa.com/ (17.03.2015).

71. U.S. Silica kodulehekülg [WWW] http://www.ussilica.com/ (17.03.2015).

72. К.М. Малина. Справочник сернокислотчика. Издание 2-ое. Москва: «ХИМИЯ»,1971.

73. Otselot.,Ltd. kodulehekülg [WWW] http://otselot.com/index.php/en/ (20.03.2015).

74. Kamenny Vek kodulehekülg [WWW] http://www.basfiber.com/ (20.03.2015).

75. Cotronics corporation kodulehekülg [WWW] https://www.**cotronics**.com/ (10.03.2015).

76. Sibelco Europe kodulehekülg [WWW] http://www.eurogrit.nl/ (16.03.2015).

77. M. Antonov. Erosion resistance of Cr_3C_2-Ni cermets at room and high temperatures, Tallinn University of Technology, 2002.

78. A. Zikin. Short review of test equipment and work processes in tribology laboratory. Tallinn University of Technology, 2010.

79. Nabertherm GmbH kodulehekülg [WWW] http://www.nabertherm.com/ (27.03.2015).

80. Robert Bosch Tool Corporation kodulehekülg [WWW] http://www.dremeleurope.com/ (29.03.2015).